

GLK Transcription Factors Coordinate Expression of the Photosynthetic Apparatus in *Arabidopsis*

Mark T. Waters,^a Peng Wang,^a Muris Korkaric,^a Richard G. Capper,^b Nigel J. Saunders,^c and Jane A. Langdale^{a,1}

^aDepartment of Plant Sciences, University of Oxford, Oxford, OX1 3RB, United Kingdom

^bOxford Gene Technology, Begbroke Science Park, Yarnton, Oxford, OX5 1PF, United Kingdom

^cSir William Dunn School of Pathology, University of Oxford, Oxford, OX1 3RE, United Kingdom

Chloroplasts of photosynthetic organisms harness light energy and convert it into chemical energy. In several land plants, GOLDEN2-LIKE (GLK) transcription factors are required for chloroplast development, as *glk1 glk2* double mutants are pale green and deficient in the formation of the photosynthetic apparatus. We show here that *glk1 glk2* double mutants of *Arabidopsis thaliana* accumulate abnormal levels of chlorophyll precursors and that constitutive *GLK* gene expression leads to increased accumulation of transcripts for antenna proteins and chlorophyll biosynthetic enzymes. To establish the primary targets of *GLK* gene action, an inducible expression system was used in combination with transcriptome analysis. Following induction, transcript pools were substantially enriched in genes involved in chlorophyll biosynthesis, light harvesting, and electron transport. Chromatin immunoprecipitation experiments confirmed the direct association of *GLK1* protein with target gene promoters, revealing a putative regulatory *cis*-element. We show that *GLK* proteins influence photosynthetic gene expression independently of the *phyB* signaling pathway and that the two *GLK* genes are differentially responsive to plastid retrograde signals. These results suggest that *GLK* genes help to coregulate and synchronize the expression of a suite of nuclear photosynthetic genes and thus act to optimize photosynthetic capacity in varying environmental and developmental conditions.

INTRODUCTION

Photosynthetic organisms rely on the efficient collection of light to drive photochemical reactions and fix inorganic carbon. The photosynthetic apparatus that harvests light comprises a series of multisubunit protein complexes that reside on convoluted, internal chloroplast membranes called thylakoids. Two of these protein complexes, photosystem I (PSI) and photosystem II (PSII), are each composed of a core reaction center surrounded by a peripheral light-harvesting complex called LHCI and LHCII, respectively. The LHC comprises protein-bound chlorophyll and carotenoid pigments that optimize light absorption and transfer excitation energy to additional chlorophylls in the reaction center (Green and Durnford, 1996).

In land plants, the genetic contribution to photosynthesis is shared between the nuclear and plastid genomes (Martin et al., 2002). The genes encoding many of the photosystem reaction center subunits are in the plastid, while those for the LHC proteins reside in the nucleus. The *Lhcb* gene family encodes members of LHCII, and the *Lhca* family encodes members of LHCI (Jansson, 1999). While chlorophyll *a* is distributed throughout the chlorophyll binding subunits of PSI and PSII, chlorophyll *b*

is uniquely bound to LHCs and not to reaction center proteins (Green and Durnford, 1996). There is much evidence suggesting that chlorophyll *b* is absolutely required for LHC assembly. First, *Arabidopsis thaliana* mutants lacking chlorophyllide *a* oxygenase (CAO) are unable to synthesize chlorophyll *b* and do not accumulate Lhcb1 to Lhcb6 (Espineda et al., 1999). Second, Lhcb proteins only insert into barley (*Hordeum vulgare*) etioplast membranes *in vitro* when supplemented with derivatives of chlorophyll *b* (Kuttkat et al., 1997). Third, CAO is necessary for the import of Lhcb monomers into isolated chloroplasts (Reinbothe et al., 2006). Thus, the concurrent events of Lhcb import, pigment binding, and protein folding mean that assembly of LHCII and chlorophyll biosynthesis are inseparable processes. Since all *Lhc* genes and all chlorophyll biosynthesis genes reside in the nucleus, it follows that these genes might be coregulated for efficient photosynthetic development. However, few examples of transcription factors that regulate chloroplast biogenesis have been described, and, to our knowledge, none have been shown to coordinate photosystem assembly *per se*.

Golden2-like (GLK) genes encode GARP nuclear transcription factors (Riechmann et al., 2000) as defined by GOLDEN2 in maize (*Zea mays*), the *Arabidopsis* RESPONSE REGULATOR-B proteins, and the PHOSPHATE STARVATION RESPONSE1 protein of *Chlamydomonas reinhardtii*. *GLK* genes have been implicated in the regulation of chloroplast development in *Arabidopsis*, *Z. mays*, and the moss *Physcomitrella patens* (Rossini et al., 2001; Fitter et al., 2002; Yasumura et al., 2005). In each species examined, *GLK* genes exist as a homologous pair named *GLK1* and *GLK2*. In moss and *Arabidopsis*, *GLK* genes are redundant and functionally equivalent, such that

¹ Address correspondence to jane.langdale@plants.ox.ac.uk.

The author responsible for distribution of materials integral to the findings presented in this article in accordance with the policy described in the Instructions for Authors (www.plantcell.org) is: Jane A. Langdale (jane.langdale@plants.ox.ac.uk).

 Online version contains Web-only data.

 Open Access articles can be viewed online without a subscription. www.plantcell.org/cgi/doi/10.1105/tpc.108.065250

only *glk1 glk2* double mutants exhibit a perturbed phenotype (Yasumura et al., 2005; Waters et al., 2008). *Arabidopsis* double mutants are pale green, and mesophyll cells contain small chloroplasts with sparse thylakoid membranes that fail to form grana. Consistent with the poorly developed chloroplasts, *glk1 glk2* mutants exhibit reduced transcript and protein levels for nuclear-encoded photosynthetic genes, especially those associated with chlorophyll biosynthesis and light harvesting (Fitter et al., 2002). Notably, however, a pale-green phenotype and the associated perturbations in chlorophyll biosynthesis and photosystem assembly could potentially result from any number of primary defects in chloroplast biogenesis. As such, the identification of immediate gene targets is necessary to further understand GLK function.

To elucidate the primary basis for the *glk1 glk2* phenotype, we further characterized the effects of the mutation on photosynthetic gene expression and on flux through the chlorophyll pathway. Using inducible gene expression combined with transcriptome analysis, we show that *GLK* genes encode transcriptional activators that promote the expression of a number of genes that are required for chlorophyll biosynthesis and light-harvesting functions. In addition, we provide evidence that *GLK1* binds directly to the promoter sequences of many of these genes and use this information to predict a *GLK cis*-element. Finally, we show that *GLK* genes regulate the expression of one of these genes independently of the phyB signaling pathway and that *GLK* genes are sensitive to plastid-derived retrograde signals. Together, these findings demonstrate that *GLK* proteins help coordinate the transcription of a suite of photosynthetic genes and suggest that *GLK* function may optimize photosynthetic capacity by integrating responses to variable environmental and endogenous cues.

RESULTS

Constitutive Expression of *GLK1* and *GLK2* Stimulates Expression of Light Harvesting and Chlorophyll Biosynthesis Genes

Several genes encoding proteins associated with light harvesting and chlorophyll biosynthesis are downregulated in *glk1 glk2* mutants (Fitter et al., 2002; Yasumura et al., 2005). To determine whether this defect can be rescued by constitutive expression of *GLK1* or *GLK2*, transcript levels were compared in wild-type, double mutant, and overexpressing plants. With respect to light harvesting, steady state transcript levels for *Lhcb1-6* are reduced in *glk1 glk2* mutants, to ~10 to 50% of the wild type (Figure 1). Overexpression of *GLK* genes fully complements this defect and notably leads to transcript levels of *Lhcb2.1* and *Lhcb3* that are approximately twofold higher than the wild type. This relationship is true for plants grown under two different light intensities. Importantly, both *glk1 glk2* mutants and *GLK* overexpressors adapt to light intensity in a similar manner to the wild type; that is, *Lhcb* transcript levels increase with the availability of light, at least at the relatively low light intensities used in this experiment and elsewhere (Ruckle et al., 2007). Thus, light intensity-dependent regulation of photosynthetic gene expression is unperturbed in *glk1 glk2* mutants.

To examine the relationship between *GLK* function and chlorophyll biosynthesis, the expression profiles of four genes regulating key enzymatic steps (Larkin et al., 2003; Tanaka and Tanaka, 2007) in the pathway were monitored: *HEMA1* (glutamyl-tRNA reductase [GluTR], which catalyzes the rate-limiting and first committed step in tetrapyrrole biosynthesis), *CHLH* (the H subunit of Mg-chelatase, which diverts tetrapyrroles toward chlorophyll biosynthesis), *GUN4* (required for efficient Mg-chelatase activity), and *CAO* (which catalyzes the conversion of chlorophyllide *a* to chlorophyllide *b*). As anticipated, transcript levels of all four genes were substantially reduced in *glk1 glk2* mutants (Figure 1). Surprisingly, however, overexpression of *GLK* genes led to transcript levels that were approximately two- to threefold higher than the wild type, an effect that was most pronounced under low light conditions (Figure 1). Consistent with the increased levels of chlorophyll observed in *GLK*-overexpressing lines (Waters et al., 2008), this finding implies that *GLK* genes promote the transcription of genes responsible for key steps in chlorophyll biosynthesis and thus may increase flux through the pathway.

Importantly, the positive effect of *GLK* overexpression on photosynthetic gene expression is not universal because transcript levels of *RbcS1* (nuclear-encoded small subunit of ribulose-1,5-bisphosphate carboxylase/oxygenase) do not differ between the four genotypes considered (Figure 1). This is consistent with the earlier report that *RbcS* transcripts are unaffected in *glk1 glk2* mutants (Fitter et al., 2002). This observation suggests that *GLK* genes primarily influence genes related to light harvesting and chlorophyll biosynthesis.

Flux through the Chlorophyll Pathway Is Compromised in Dark-Grown *glk1 glk2* Mutants

While the *glk1 glk2* phenotype is readily observable in light-grown plants, it is not known whether *GLK* genes are required for chloroplast development in the absence of light. Etiolated seedlings do not synthesize chlorophyll, but instead prepare for eventual light exposure by accumulating large quantities of protochlorophyllide (Pchl) in developmentally arrested plastids called etioplasts. In the etioplast stroma, the accumulated Pchl, together with NADPH:Pchl oxidoreductase, forms a crystalline array called the prolamellar body (Sundqvist and Dahlin, 1997). To establish whether plastids of dark-grown *glk1 glk2* mutants are phenotypically distinguishable from those of the wild type, we examined the ultrastructure of cotyledon etioplasts. While still exhibiting a crystalline appearance, the prolamellar bodies of *glk1 glk2* etioplasts were smaller than those of the wild type, invariably occupying less of the stroma (Figures 2A and 2B). Wild-type and mutant prolamellar bodies exhibited a mean width of $1.62 \pm 0.06 \mu\text{m}$ and $1.06 \pm 0.08 \mu\text{m}$, respectively, when measured at the widest point ($n = 12$). This observation implies that *glk1 glk2* mutants accumulate lower levels of chlorophyll precursors, even in the dark.

Consequently, we measured levels of chlorophyll precursors in dark-grown seedlings by spectrofluorometry. Figure 2C shows that levels of Pchl are reduced in *glk1 glk2* mutants, implying that *GLK* function is required for normal Pchl synthesis in the dark. This observation, in combination with the reduced

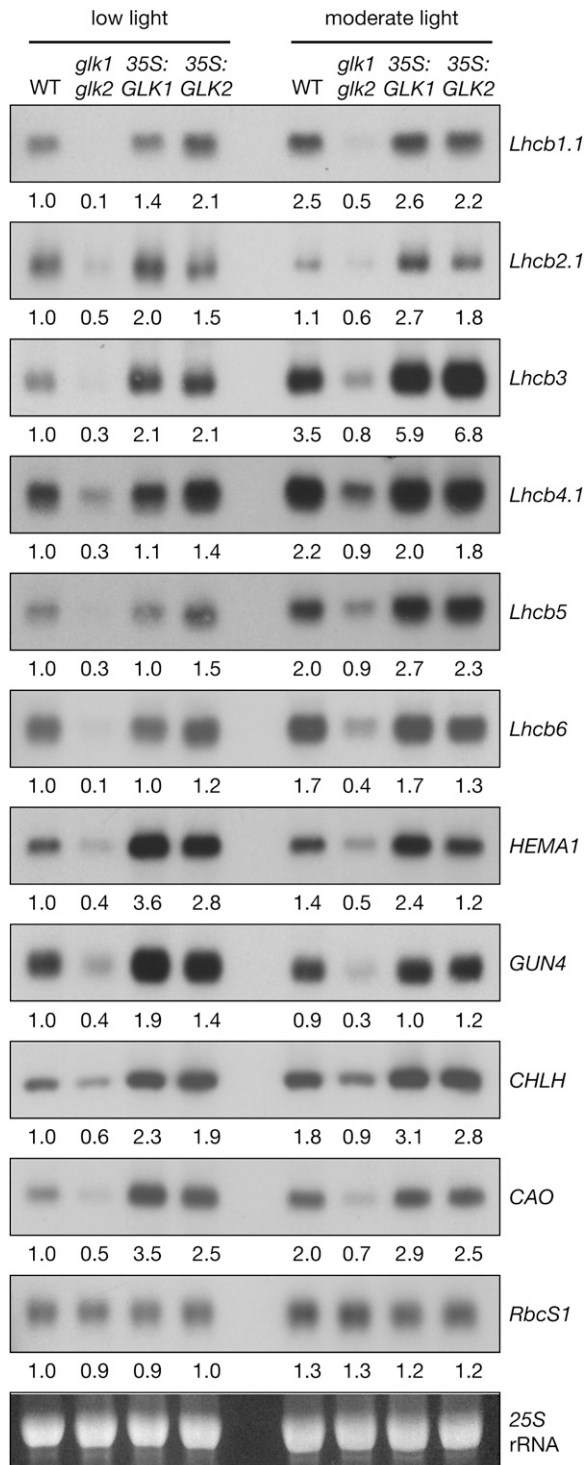


Figure 1. Overexpression of *GLK* Genes Leads to Enhanced Transcript Levels of Nuclear Photosynthetic Genes.

RNA gel blot analysis showing transcript levels in wild-type, double mutant (*glk1 glk2*), and double mutant lines overexpressing either *GLK1* (35S:*GLK1*) or *GLK2* (35S:*GLK2*). Plants were grown for 28 d under 30 or 100 $\mu\text{mol quanta}\cdot\text{m}^{-2}\cdot\text{s}^{-1}$ (low light and moderate light, respectively) at 21°C. All tissue samples were harvested within 20 min, starting at 3 h

accumulation levels of transcripts encoded by chlorophyll biosynthesis genes (Figure 1), suggested that loss of *GLK* function might reduce flux through the entire pathway. To test this suggestion, we fed dark-grown seedlings with 5-aminolevulinic acid (ALA), an early tetrapyrrole precursor. Excitation at 420 nm produces an emission peak at 595 nm corresponding to Mg-Protoporphyrin IX (Mg-ProtoIX) and/or Mg-Protoporphyrin IX methyl ester (Mg-ProtoIX ME) (Pontier et al., 2007). Notably, feeding with ALA increased the 595-nm peak in *glk1 glk2* relative to the wild type (Figure 2C), implying reduced activity of Mg-ProtoIX methyltransferase and/or Mg-ProtoIX ME cyclase in the mutant. In addition, excitation at 440 nm produced a 632-nm emission peak, contributed mainly by Pchl_a, that was almost equalized between *glk1 glk2* and the wild type upon feeding with ALA (see Supplemental Figure 1 online). This result suggests that decreased ALA synthesis might be also responsible for the decreased Pchl_a levels in the mutant.

We further fed dark-grown seedlings with 2,2'-dipyridyl (DP). DP inhibits the conversion of ProtoIX to heme and also the conversion of Mg-ProtoIX to Pchl_a, thus leading to the accumulation of Mg-ProtoIX and Mg-ProtoIX ME (Mochizuki et al., 2001; see also Figure 4). As expected, feeding with DP led to reduced amounts of Pchl_a in both the wild type and *glk1 glk2* (see Supplemental Figure 1 online), but it also produced a large increase in Mg-ProtoIX and/or Mg-ProtoIX ME levels in the mutant relative to the wild type (Figure 2C). Since DP inhibition is presumed to occur immediately after Mg-ProtoIX ME, the different increases in the 595-nm peak suggest that at least Mg-ProtoIX was accumulating in the mutant. Moreover, excitation at 400 nm (which is specific for ProtoIX) led to a higher emission peak at 632 nm in the mutant than in the wild type (Figure 2C) that was not seen when excitation was performed at 440 nm (see Supplemental Figure 1 online).

This suggests that ProtoIX also accumulates to higher levels in the mutant than the wild type when treated with DP. The elevated accumulation of ProtoIX and Mg-ProtoIX is consistent with the reduced levels of *GUN4* and *CHLH* transcripts and those of *CHLM* (encoding Mg-ProtoIX methyltransferase), as implied by the transcriptome analysis below. Additionally, decreased levels of heme and/or Pchl_a in mutant seedlings may depress negative feedback of GluTR, either directly or via FLU, a negative regulator of chlorophyll biosynthesis (Terry and Kendrick, 1999; Meskauskiene et al., 2001; Goslings et al., 2004). This effect would further enhance levels of ProtoIX and Mg-ProtoIX relative to the wild type when treated with DP. Together, these findings indicate a general reduction of flux through the chlorophyll pathway in *glk1 glk2* mutants and imply that *glk1 glk2* mutants process ProtoIX and Mg-ProtoIX at a slower rate than the wild type.

after subjective dawn. Ten micrograms of total RNA was loaded per lane. Blots were exposed to a phosphor-imager screen for quantification; images shown are subsequent exposures to autoradiography film. Values below each blot denote the approximate fold-change relative to the wild type grown under low light, standardized to 25S rRNA on the ethidium bromide-stained gel.

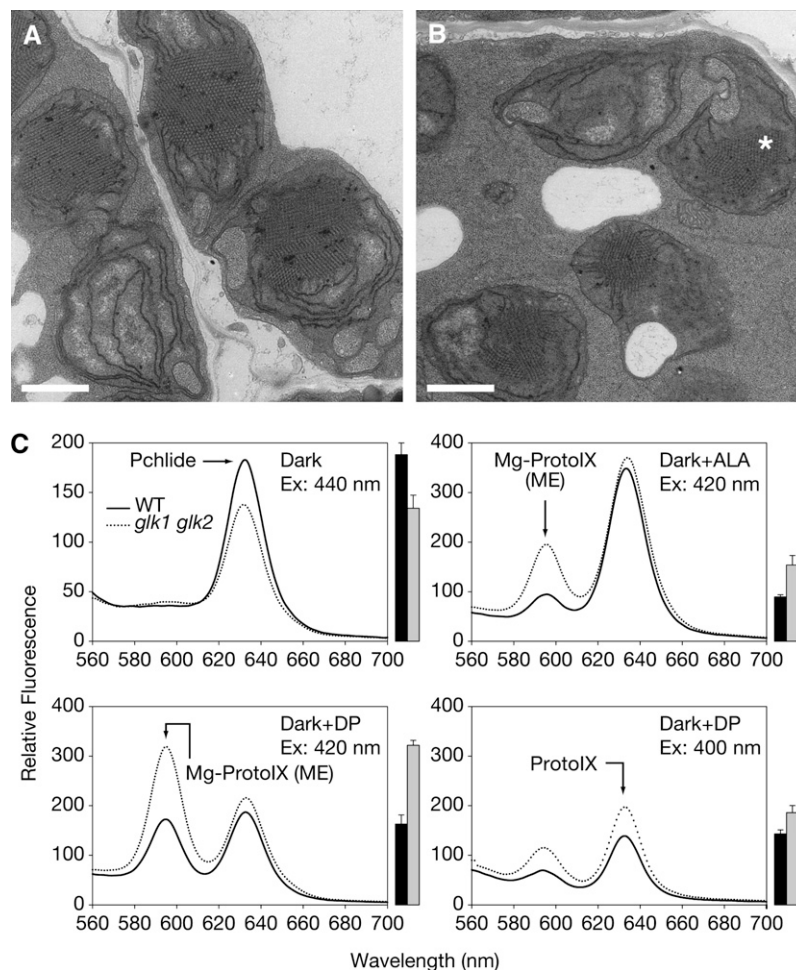


Figure 2. Dark-Grown *glk1 glk2* Seedlings Exhibit Defects in the Chlorophyll Biosynthetic Pathway.

(A) and (B) Transmission electron micrographs of etioplasts in the cotyledons of dark-grown 4-d-old wild type (A) and *glk1 glk2* seedlings (B). Asterisk denotes the prolamellar body. Bars = 1 μ m.

(C) Levels of chlorophyll intermediates in dark-grown wild-type and *glk1 glk2* seedlings as determined by spectrofluorometry. Top left panel: untreated seedlings. Excitation at 440 nm produces an emission peak at 632 nm corresponding to Pchlde. Top right panel: seedlings treated with 10 mM ALA. Excitation at 420 nm produces an emission peak at 595 nm corresponding to MgProtoIX (ME) and an additional, nonspecific peak at 632 nm corresponding to Pchlde and protoporphyrin IX (ProtoIX) (Pontier et al., 2007). Bottom panels: seedlings treated with 10 mM DP. In the bottom right panel, excitation at 400 nm produces an emission peak at 632 nm corresponding to ProtoIX. Bars to the right of each chart show quantification of the arrowed peak (mean \pm SE, $n = 3$ biological replicates). The wild type is represented with black bars and *glk1 glk2* with gray bars.

Induction of *GLK1* and *GLK2* Leads to Increased Levels of Chlorophyll

To gain insight into the targets of GLK transcription factors, we designed an experiment where expression of *GLK1* or *GLK2* could be induced in a *glk1 glk2* mutant background. The aim was to measure transcriptome changes following induction. A two-component glucocorticoid-inducible system was used to drive *GLK1* or *GLK2* expression following treatment with dexamethasone (DEX) (Craft et al., 2005). Briefly, the *GLK1* and *GLK2* coding sequences were cloned behind a chimeric promoter consisting of a minimal cauliflower mosaic virus 35S promoter and six ideal *lac* operator sequences, termed *pOp6* (Kannangara et al., 2007). These constructs were then independently trans-

formed into a transgenic *glk1 glk2* line carrying a transcriptional activator LhGR-N driven by a constitutively active 35S promoter. Application of DEX facilitates entry of LhGR-N into the nucleus and consequent activation of transcription from the *pOp6* promoter. This method requires subsequent translation of *GLK* mRNA and therefore precludes the inhibition of protein synthesis when monitoring for downstream transcriptional changes.

The progeny of primary transformants carrying *pOp6:GLK1* or *pOp6:GLK2* were first screened for their capacity to induce *GLK* expression following application of DEX. DEX (10 μ M) was sufficient to induce a strong transcriptional response when plants were grown on media containing the hormone, and induced plants contained significantly more chlorophyll than uninduced siblings (see Supplemental Figure 2 online). However,

chlorophyll levels were still substantially lower than the wild type, implying that induced expression was insufficient to fully rescue the mutant phenotype. Although both inducible constructs encoded a C-terminal FLAG epitope tag, we were unable to detect *GLK1* or *GLK2* proteins following induction, consistent with the reported protein instability (Waters et al., 2008).

To confirm that *GLK*-FLAG fusion proteins are indeed functional, identical coding sequences were expressed from the cauliflower mosaic virus 35S promoter. Significantly, these constructs fully complemented the *glk1 glk2* mutant phenotype (see Supplemental Figure 3 online). The incomplete phenotypic rescue by *pOp6:GLK1/GLK2* is unlikely to be caused by low transcript abundance, as levels were substantially higher than the wild type (see Supplemental Figure 4 online). Instead, it may reflect a developmental window when *GLK* expression is fundamentally required and/or a location that may not be accessible to DEX, such as young leaf primordia. Because at least partial complementation was possible, the most strongly induced transgenic line for each of *pOp6:GLK1* and *pOp6:GLK2* (line T₂3 for both; see Supplemental Figure 2 online) was selected for subsequent microarray experiments.

To determine the optimal time for induction, *GLK1* and *GLK2* transcript levels were measured over time after DEX application. Seedlings were germinated on agar plates and 10 d later were transferred to liquid medium and allowed to recover for 48 h. Induction was achieved by adding 10 μ M DEX. *GLK1* and *GLK2* transcripts were detectable within 1 h of induction and reached a maximum within 4 to 8 h (see Supplemental Figure 4 online). On the basis of these kinetics, we reasoned that a 4-h induction period would allow sufficient time for *GLK* accumulation (both RNA and protein) and activation of direct targets, while minimizing secondary indirect effects associated with longer induction periods.

***GLK1* and *GLK2* Upregulate Similar Genes**

To analyze the genome-wide effects on transcription following *GLK* induction, microarray experiments were performed on four independent biological replicates for each of *pOp6:GLK1* and *pOp6:GLK2*. Following RNA extraction, we confirmed induction of *GLK1* or *GLK2* transcripts in each sample by RNA gel blot analysis. Within each line, all four replicates showed strong and consistent induction, although *pOp6:GLK1* induced approximately sixfold more strongly than *pOp6:GLK2* (Figure 3A). Strikingly, microarray analysis revealed that *GLK1* and *GLK2* upregulate very similar sets of genes (Figures 3B and 3C). Responsive genes were identified using a stringent significance threshold: a mean fold change ≥ 2 (induced relative to uninduced samples) and a P value ≤ 0.01 , based on at least three out of the four replicates.

When ranked by mean fold change, the 20 most affected genes following *GLK2* induction were also significantly induced by *GLK1*; most prominent in this list were *Lhcb* and chlorophyll biosynthesis genes (Figure 3B). These 20 genes tended to show a stronger response in *pOp6:GLK1* samples than *pOp6:GLK2* samples, likely reflecting the difference in induction strength in these two lines (Figure 3A). Consistent with this inference, 114 genes satisfied the significance threshold and were upregulated in response to *GLK1*, compared with 47 for *GLK2*. Of these 47

genes, 40 were also upregulated by *GLK1* (Figure 3C), and of the seven excluded genes, five were omitted from the *GLK1* list based solely on a fold ratio marginally < 2 (see Supplemental Tables 1 and 2 online).

When the data sets of *GLK1* and *GLK2* are combined, the similarity in upregulated genes becomes most evident and the changes are highly statistically significant (Table 1; see Supplemental Table 3 online). By contrast, only 10 and three genes were downregulated by *GLK1* and *GLK2*, respectively, using the same significance threshold (see Supplemental Tables 4 and 5 online). Furthermore, none of these genes was consistently downregulated by both *GLK1* and *GLK2*. Together, these data suggest that *GLK1* and *GLK2* promote the expression of highly similar genes, consistent with their known functional equivalency.

***GLK*-Regulated Genes Are Primarily Involved in Photosynthetic Function**

Genes significantly upregulated by *GLK1* were categorized according to the predicted or known subcellular location of their gene products. Of 114 proteins, 66 could be unambiguously localized to a cellular compartment based on annotation or computational prediction using WoLF PSORT (Horton et al., 2007). Approximately half of these proteins were localized to the chloroplast, a further half of which were thylakoid proteins (Figure 3D). When classified according to known or predicted molecular function, 27 of 71 genes were involved in photosynthesis or chloroplast function, with a further 18 and 14 involved in general metabolism and transcription, respectively (Figure 3E).

To assess the degree to which these classifications are over-representative of *Arabidopsis* proteins as a whole, the *GLK1*-upregulated genes were submitted to enrichment analysis using the DAVID Functional Annotation tool (Huang et al., 2007). When classified according to Gene Ontology (GO) terms relating to biological process, cellular compartment, and molecular function, photosynthesis-related terms are by far the most highly represented and are highly significantly enriched (Table 2). The three most enriched biological processes (protein-chromophore linkage, photosynthesis, light harvesting, and chlorophyll biosynthetic process) imply that *GLK* genes promote the expression of nuclear genes relating both to Lhcb assembly and chlorophyll biosynthesis.

Besides genes known to be directly involved in photosynthesis, several upregulated genes were identified whose products are either targeted to the chloroplast or involved in chloroplast regulatory processes. These include two related cold-responsive proteins targeted to the chloroplast stroma (COR15a and b), two rhodanese-like domain-containing proteins targeted to the thylakoid lumen, and CIA2, a nuclear transcription factor involved in the expression of two components of the plastid protein import complex (Sun et al., 2001). In addition, a nuclear-encoded chloroplast RNA polymerase σ -subunit was upregulated by both *GLK1* and *GLK2*. This protein is required for the expression of chloroplast-encoded photosynthetic proteins and tRNAs, including tRNA^{Glu}, an early intermediate in the tetrapyrrole biosynthesis pathway (Hanaoka et al., 2003). Interestingly, phytoene synthase was also significantly upregulated, which is consistent with the need for carotenoid biosynthesis during LHC assembly.

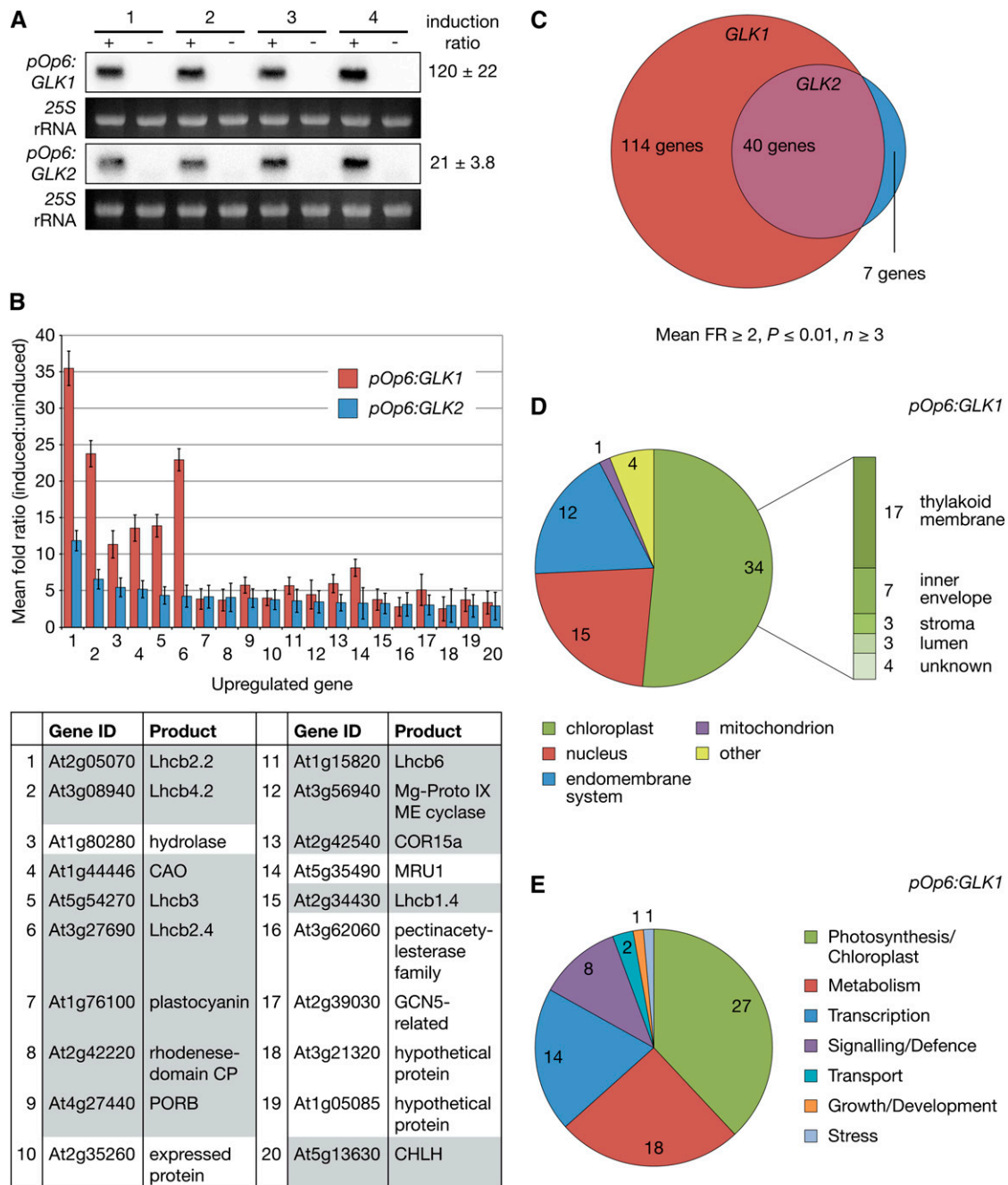


Figure 3. Induction of *GLK* Expression Promotes Transcription of Photosynthesis-Related Genes.

(A) RNA gel blot showing *GLK1* and *GLK2* transcript accumulation following induction. Four independent biological replicates (1 to 4) of seedlings carrying *pOp6:GLK1* or *pOp6:GLK2* transgenes were grown under a 16-h-light/8-h-dark cycle, induced 6 h after dawn with 10 μ M DEX (+) or mock-treated with 0.1% DMSO (–), and then harvested 4 h later. Five micrograms of total RNA was loaded in each lane, and hybridization was quantified using a phosphor-imager. The induction ratio is calculated as (induced value)/(mock value) and expressed as a mean \pm SE ($n = 4$).

(B) The mean fold ratio for the 20 most upregulated genes following *GLK2* induction (blue) is plotted alongside the mean fold ratio for the same genes following *GLK1* induction (red). Note that the *GLK1*-induced genes are generally more strongly affected than *GLK2*-induced genes. Error bars are SD ($n \geq 3$ biological replicates). The table lists the 20 genes depicted in the chart; shaded cells correspond to photosynthetic/chloroplast-localized gene products and are described in the text. Supplemental Table 2 online lists all genes significantly changed in response to *GLK2* induction and therefore lists the details of these top 20 genes.

(C) The number of upregulated genes shared between induced *pOp6:GLK1* and *pOp6:GLK2* samples are represented by overlapping circles, the areas of which are proportional to the number of genes that pass the significance threshold.

Table 1. Twenty Most Upregulated Genes following Induction of *GLK1* and *GLK2*

Gene ID	Name	Location ^a	GLK1 mFR ^b	GLK1 P Value	<i>n</i> ^c	GLK2 mFR ^b	GLK2 P Value	<i>n</i> ^c	Comb. mFR ^d	Comb. P Value	<i>n</i> ^c
At2g05070	Lhcb2.2	Thy.	35.5	3.71E-08	3	11.8	2.79E-08	4	19.0	1.50E-09	7
At3g08940	Lhcb4.2	Thy.	23.8	5.71E-09	4	6.5	5.93E-07	4	12.5	2.03E-09	8
At3g27690	Lhcb2.4	Thy.	22.9	4.52E-10	4	4.2	7.26E-06	4	9.9	7.85E-08	8
At1g80280	Hydrolase, α - β	PM?	11.3	6.02E-08	4	5.4	3.67E-07	4	7.9	1.83E-09	8
At1g44446	CAO	IE	13.6	8.57E-08	3	5.2	5.51E-07	4	7.9	6.95E-09	7
At5g54270	Lhcb3	Thy.	13.9	1.70E-09	4	4.3	9.97E-07	4	7.8	2.37E-08	8
At5g35490	MRU1 (unknown)	Mit.?	8.1	7.36E-08	4	3.3	3.87E-03	3	5.5	1.14E-06	7
At5g48490	LTP (unknown lipid transfer protein)	endo.?	8.6	3.88E-09	4	2.7	1.16E-04	4	4.8	5.07E-07	8
At4g27440	Protochlorophyllide oxidoreductase (PORB)	IE	5.7	5.39E-10	4	3.9	1.33E-04	4	4.8	4.45E-10	8
At1g15820	Lhcb6	Thy.	5.7	1.61E-06	4	3.6	2.20E-04	4	4.5	1.02E-07	8
At2g42540	COR15a	Str.	5.9	1.22E-05	3	3.3	1.57E-04	4	4.3	1.70E-07	7
At1g76100	Plastocyanin	Lum.	3.8	2.41E-06	4	4.1	2.71E-05	4	4.0	1.24E-08	8
At2g39030	GNAT family	?	5.1	1.88E-05	4	3.0	2.13E-04	4	3.9	7.86E-07	8
At3g56940	Mg-proto IX ME cyclase (<i>CRD1</i>)	IE	4.4	3.44E-05	4	3.4	3.03E-04	4	3.9	1.40E-06	8
At2g42220	Rhodanese-like domain	Thy.	3.7	3.26E-06	4	4.1	7.83E-05	4	3.9	1.64E-07	8
At2g35260	Expressed protein	?	4.0	2.25E-06	4	3.7	2.43E-04	4	3.9	6.58E-09	8
At2g34430	Lhcb1.4	Thy.	3.8	3.06E-05	4	3.2	6.34E-05	4	3.5	2.63E-08	8
At4g05180	PsbQ2	Thy.	4.6	3.24E-06	4	2.6	1.11E-04	4	3.5	3.45E-08	8
At1g68190	Zinc finger family	Nuc.	4.3	7.08E-06	4	2.7	3.15E-04	4	3.4	1.84E-06	8
At1g05085	Hypothetical protein	?	3.7	9.19E-04	3	2.9	8.64E-04	4	3.2	8.97E-06	7

Ranked by combined fold ratio across both *GLK1* and *GLK2* data sets.

^aThy., thylakoid membrane; lum., thylakoid lumen; IE, chloroplast inner envelope; str, chloroplast stroma; mit., mitochondrion; endo., endomembrane system; nuc., nucleus; ?, unknown/uncertain.

^bMean fold ratio of signal (induced:mock-treated).

^cNumber of independent observations (arrays scored).

^dCombined fold ratio across both *GLK1* and *GLK2* data sets.

Key Steps of the Chlorophyll Pathway Are Upregulated following *GLK* Induction

Given that chlorophyll biosynthesis is clearly perturbed in *gk1 gk2* double mutants, we identified genes corresponding to each step in tetrapyrrole and chlorophyll biosynthesis and assessed how transcript levels changed in response to *GLK1* and *GLK2* induction. This approach revealed five key steps that are influenced by *GLK1* and *GLK2* induction (Figure 4; see Supplemental Table 6 online). The tetrapyrrole pathway starts with the generation of glutamate 1-semialdehyde and branches at ProtoIX. At this point, ProtoIX is diverted toward either chlorophyll or heme biosynthesis by the chelation of Mg²⁺ or Fe²⁺, respectively. As expected, *HEMA1* was significantly upregulated, but no other steps prior to Proto IX were affected. The branch toward chlorophyll, catalyzed by Mg-cheletase, was strongly promoted:

both *CHLH* and *GUN4* registered significant increases (Figure 4). Interestingly, expression of the two other subunits of Mg-cheletase, *CHLD* and *CHLI*, was unchanged, a finding consistent with other work, indicating that transcriptional regulation of this step is achieved through *CHLH* and *GUN4* (Matsumoto et al., 2004; Stephenson and Terry, 2008).

Most notably, genes encoding Fe-cheletase and downstream heme biosynthetic enzymes were unaffected, suggesting a specific upregulation of the chlorophyll branch of the pathway. Thereafter, three major steps were upregulated by *GLK* induction: (1) the generation of divinylprotochlorophyllide *a*, a three-step reaction that requires Mg-ProtoIX monomethylester cyclase (*CRD1*); (2) the generation of chlorophyllide *a* by Pchlde oxidoreductase (*PORA*, *PORB*, and *PORC*); and (3) the oxidation of chlorophyllide *a* to chlorophyllide *b* by CAO. The upregulation of *CRD1* is consistent with the observation that mutant plants

Figure 3. (continued).

(D) Subcellular and subchloroplastic localization of gene products induced by *GLK1*. Gene products were assigned a location based on GO annotation. If unknown, the location was predicted by WoLF PSORT and assigned a location if this prediction was unambiguous. Unknown or ambiguous locations were excluded. GO annotations and assigned locations are listed in Supplemental Table 1 online.

(E) Functional characterization of gene products induced by *GLK1*. Gene products were assigned a function based on GO annotation. GO annotations and assigned functions are listed in Supplemental Table 1 online.

Table 2. Functional Enrichment of *GLK1*-Induced Genes

Term ID	Term	Count ^a	% ^b	FE ^c	P Value ^{d,e}
	GO: Biological Process (BP)				
GO:0015979	Photosynthesis	15	13.51	25.47	4.29E-16
GO:0009765	Photosynthesis, light harvesting	10	9.01	58.35	7.26E-14
GO:0018298	Protein-chromophore linkage	5	4.50	61.72	1.13E-06
GO:0006091	Generation of precursor metabolites and energy	17	15.32	3.99	2.32E-06
GO:0015995	Chlorophyll biosynthetic process	5	4.50	44.58	4.36E-06
GO:0015994	Chlorophyll metabolic process	5	4.50	35.66	1.08E-05
GO:0046148	Pigment biosynthetic process	6	5.41	20.06	1.13E-05
GO:0033014	Tetrapyrrole biosynthetic process	5	4.50	23.60	5.61E-05
	GO: Cellular Compartment (CC)				
GO:0009579	Thylakoid	22	19.82	14.34	7.51E-19
GO:0044434	Chloroplast part	19	17.12	11.26	2.79E-14
GO:0031984	Organelle subcompartment	16	14.41	14.17	2.23E-13
GO:0042651	Thylakoid membrane	15	13.51	16.07	2.93E-13
GO:0009507	Chloroplast	33	29.73	3.59	1.44E-11
GO:0009522	PSI	6	5.41	52.14	8.46E-08
GO:0009523	PSII	7	6.31	24.51	3.58E-07
GO:0031090	Organelle membrane	16	14.41	4.95	4.33E-07
GO:0043231	Intracellular membrane-bound organelle	46	41.44	1.46	5.38E-04
	GO: Molecular Function (MF)				
GO:0016168	Chlorophyll binding	4	3.60	131.50	3.19E-06
GO:0000287	Magnesium ion binding	6	5.41	8.77	5.66E-04
GO:0016628	Oxidoreductase activity	3	2.70	42.27	2.22E-03
GO:0030528	Transcription regulator activity	13	11.71	2.66	2.56E-03
GO:0046906	Tetrapyrrole binding	6	5.41	5.80	3.48E-03
GO:0003700	Transcription factor activity	11	9.91	2.81	4.57E-03
GO:0016630	Protochlorophyllide reductase activity	2	1.80	197.25	9.94E-03

A total of 114 genes were submitted to the DAVID Functional Enrichment Chart tool, resulting in 111 unique gene IDs. Terms are ranked by significance of overrepresentation.

^aNumber of submitted genes with GO term.

^bProportion of submitted genes with GO term.

^cRelative fold enrichment (FE) of GO term compared with *Arabidopsis* gene background.

^dSignificance of fold enrichment (FE), given by a modified Fisher Exact test (Hosack et al., 2003).

^eTerms were included in list if $P < 0.001$ for BP and CC, or $P < 0.01$ for MF.

accumulate Mg-ProtoIX following addition of ALA (Figure 2), indicative of a block in CHLM or CRD1 activity. The particularly pronounced upregulation of CAO transcript levels, with an average of 7.9-fold increase following *GLK* induction (Figure 4, Table 1), is similarly consistent with the link between chlorophyll *b* and *Lhcb* stability, and the substantially induced expression of *Lhcb* genes by *GLK1* and *GLK2*.

Light-Harvesting Antenna Proteins Are Significantly Upregulated by *GLK1*

Five of the 10 most upregulated genes following *GLK1* and *GLK2* induction encode subunits of LHCII (Table 1). Considering that *GLK1* induction yielded the most dramatic transcriptional changes, we examined the response of all nuclear genes encoding subunits of PSII, PSI, and the associated antennae, LHCII and LHCI (Figure 5; see Supplemental Table 7 online). In *Arabidopsis*, 10 individual genes in three classes (*Lhcb1.x*, *Lhcb2.x*, and *Lhcb3*) encode the trimeric LHCII, and a total of five genes in three classes (*Lhcb4.x*, *Lhcb5*, and *Lhcb6*) encode the peripheral minor antenna proteins. As anticipated, at least

one gene family member corresponding to each of the six subunits of the light-harvesting antenna of PSII was significantly upregulated, some of them dramatically so. Intriguingly, not all gene members within the same class responded equivalently: while *Lhcb4.2* increased 24-fold, *Lhcb4.1* only increased 1.8-fold, whereas *Lhcb4.3* showed no significant change (see Supplemental Table 7 online). An extensive metastudy of *Lhc* transcript profiles revealed subtly different patterns of expression between *Lhc* family members; notably, *Lhcb2.1* and *Lhcb2.2* share a similar tissue-specific expression profile distinct from *Lhcb2.3*, and *Lhcb4.3* is weakly expressed relative to *Lhcb4.1* and *Lhcb4.2* except in pedicels (Klimmek et al., 2006). The functional basis for this distinction is not obvious, but these differences are consistent with the responses to *GLK* genes described here.

Expression of the six *Lhca* genes encoding the PSI antenna was more moderately stimulated by *GLK1*: only two subunits surpassed the significance threshold, and expression levels increased less than threefold. Only one nuclear-encoded subunit of the PSII core complex responded robustly to *GLK1* induction: *PsbQ-2*. *PsbQ* is an extrinsic protein that forms part of the

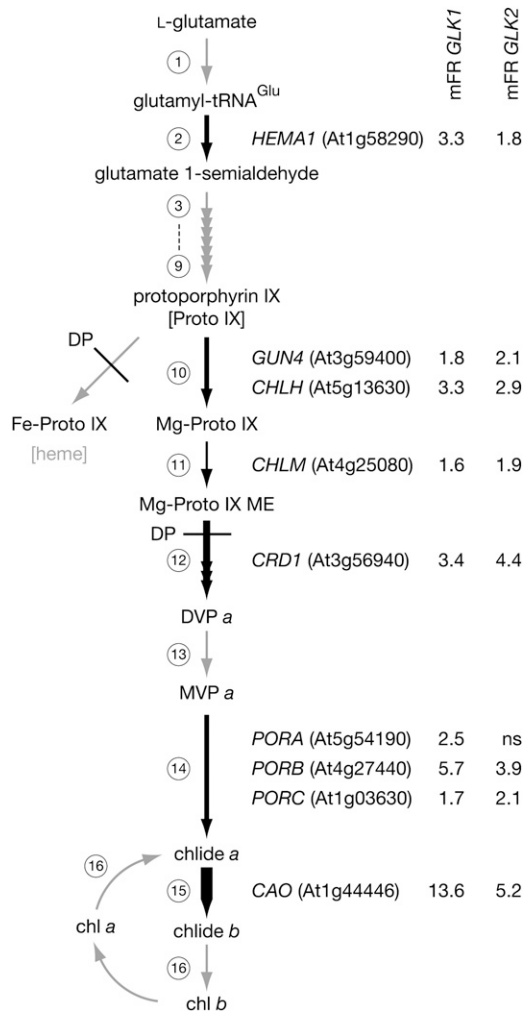


Figure 4. Effect of *GLK1* and *GLK2* Induction on the Chlorophyll Biosynthetic Pathway.

Schematic of the chlorophyll biosynthetic pathway with steps with significant changes in gene transcript levels following GLK induction depicted with black arrows; the relative strength of induction is reflected in the thickness of the arrow. Nonsignificantly changed steps and pathways are depicted with gray arrows. Values represent the mean fold ratio (mFR) change in gene expression (induced relative to non-induced) following induction of *GLK1* and *GLK2*. For clarity, only genes with significantly changed transcript levels are shown for each step. Significance threshold of $P \leq 0.05$, $n \geq 3$ biological replicates. ns, not significant. Circled numbers refer to enzymatic steps listed in Supplemental Table 6 online, which details the changes in all genes involved in this pathway. Steps inhibited by DP are also shown. The genes are *HEMA1*; *GUN4*; *CHLH*; *CHLM*, Mg-protoporphyrin IX methyl transferase; *CRD1*, Mg-protoporphyrin IX monomethyl ester cyclase; *PORA/PORB/PORC*, protochlorophyllide oxidoreductase A/B/C; *CAO*; MgProtoME, magnesium protoporphyrin monomethyl ester; *DVP*, divinylprotochlorophyllide; and *MVP*, monovinylprotochlorophyllide.

oxygen-evolving complex and is necessary for PSII stability under light-limiting conditions (Yi et al., 2006). Likewise, changes in core complex subunits of PSI were relatively weak with *PsaD* and *PsaK* upregulated two- to threefold. Beyond sustaining PSI function, the role of *PsaD* is unclear (Haldrup et al., 2003); however, *PsaK* appears to interact with LHCI and may stabilize the association of LHCI with the PSI core complex (Jensen et al., 2000). The luminal electron carrier plastocyanin was also stimulated by *GLK1* expression, perhaps reflecting the increased electron flow associated with enhanced light interception by LHC antennae.

Induction of *GLK* Expression Leads to Sustained Increases in Photosynthetic Gene Expression

To verify the microarray results, we assessed the accumulation of transcripts corresponding to several photosynthetic genes over a 24-h period following *GLK1* and *GLK2* induction (Figure 6). In general, transcripts responded more strongly to *GLK1* than *GLK2*, as suggested by the microarray data and the *GLK1* and *GLK2* induction profiles (Figures 3 and 6). Unambiguous evidence of increased transcript levels was visible 4 h after induction, with some genes showing increases after just 2 h (e.g., *GUN4* and *CAO*). In agreement with the microarray data, the most dramatically affected transcripts were those for *Lhcb1.1* and *Lhcb6*. While transcript levels in induced samples tended to peak at 4 to 8 h, concomitant with *GLK* transcript levels, levels remained elevated relative to the uninduced controls after 24 h. Importantly, transcripts for *RbcS1* remained stable throughout the 24-h time course. On the basis of these data, we conclude that the *GLK*-induced changes observed by microarray analysis are valid.

GLK Proteins Bind to Promoters of Several Photosynthetic Genes

To assess whether the upregulated genes identified by the microarray analysis are directly influenced by *GLK* activation, chromatin immunoprecipitation (ChIP) assays were performed with nuclear extracts from 35S:*GLK1* plants and antibodies raised against *GLK1*. PCR amplification revealed that the population of immunoprecipitated DNA contained promoter sequences of the genes that were most significantly upregulated in the transcriptome analysis (Figure 7). Notably, promoters of all six classes of the *Lhcb* gene family, several chlorophyll biosynthesis genes, and two genes of unknown function were confirmed as interacting with *GLK1*. However, no reliable interaction could be confirmed for *COR15a*, even though it was strongly induced, which may suggest this gene is not a direct *GLK1* target. Importantly, no enrichment for promoter sequences corresponding to two uninduced genes (*DVR* [divinyl Pchlide reductase] and *actin*) could be detected using this method. These data are consistent with *GLK1* acting as a positive transcriptional regulator of several functionally related genes through direct binding to promoter sequences. It is noteworthy that constitutive overexpression of individual photosynthetic genes (*HEMA1*, *CAO*, *Lhcb1*, and *Lhcb6*) that are otherwise downregulated in *glk1 glk2* mutants has no discernible effect on

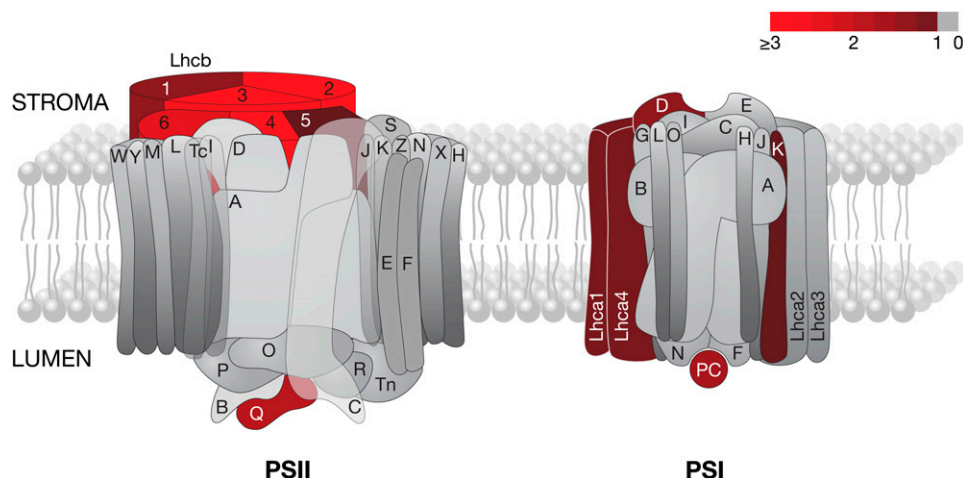


Figure 5. Thylakoid-Associated Photosynthetic Components Significantly Upregulated following Induction of *GLK1*.

Pictorial representation of PSI and PSII. The color scale depicts fold ratio in \log_2 units; a \log_2 fold ratio of 1 is equivalent to an absolute fold change of 2. Subunits showing a robust increase (>1) in corresponding transcript levels are highlighted in shades of red, with unchanged subunits in gray (<1). The significance threshold was $P \leq 0.01$ ($n \geq 3$). Note that only transcripts for nuclear-encoded proteins could be detected on the microarrays used. Subunits of PSI and PSII are referred to as Psa \S and Psb \S , respectively, where \S corresponds to the lettered labels in the figure. PC, plastocyanin. Gene IDs, significance levels, and mean fold ratios in absolute units for each subunit are listed in Supplemental Table 7 online. Figure redrawn with permission from J. Nield following the scheme at <http://photosynthesis.sbcs.qmul.ac.uk/nield/psliimages/oxygenicphotosynthmodel.html> (accessed September 2, 2008).

the mutant phenotype (see Supplemental Figure 5 online). This further implies that the *glk1 glk2* mutant phenotype is due to multiple defects in photosynthetic development.

Promoter Analysis of ChIP Targets Reveals a Putative GLK *cis*-Element

To examine whether the promoters of GLK-regulated genes share a common *cis*-element, we analyzed the 23 ChIP-positive genes using Weeder, a program that uses a consensus-based method to search for conserved motifs in submitted sequences (Pavesi et al., 2004; Tompa et al., 2005). The evaluation of any motif assesses the frequency and conservation found among the submitted sequences and compares those values to those expected given the nucleotide distributions in upstream sequences of *Arabidopsis* genes. Submitting 500 bases of sequence upstream of the annotated transcriptional start site of the 23 genes yielded a 6-bp motif, CCAATC, that was widely distributed, well conserved, and significantly overrepresented (Weeder Score 1.13; $P < 0.001$; Figure 8). While most instances of the motif contained one substitution, eight of the promoters contained one perfect instance, and three promoters contained two (Figure 8; see Supplemental Table 9 online). In addition, the G-box element (CACGTG), a ubiquitous element found in functionally diverse genes (Menkens et al., 1995), was significantly overrepresented (Weeder score of 0.99; $P < 0.001$) but was less common than CCAATC (Figure 8B). A high-scoring eight-base motif was also discovered (GCCACGTG), but this is essentially an extended G-box.

To verify that the CCAATC motif is overrepresented in GLK targets specifically, we examined the promoters of 29 photo-

synthetic genes that are not GLK targets. These included genes encoding Calvin cycle enzymes as well as chlorophyll biosynthesis genes and PSII subunit genes that were unchanged in the transcriptome analysis (see Supplemental Table 9 online). On the basic assumption that any given six-base motif will occur once every 4^6 (4096) bases, we observed that CCAATC arose in the non-GLK target promoters no more often than would be expected by chance (Figure 8B). The G-box, meanwhile, occurred more frequently than expected by chance and was more common than CCAATC. Furthermore, CCAATC was not identified as a potential motif by Weeder in these non-GLK targets. Therefore, we tentatively assign CCAATC as a putative GLK recognition sequence.

Extensive efforts to define experimentally the GLK1 binding site have proved unsuccessful. Screens of a random oligo-based library in a bacterial-1-hybrid system (Meng et al., 2005) revealed that while a GLK1 bait transactivates reporter constructs at a level significantly above background, no strong consensus sequence can be identified in recovered clones (data not shown). Furthermore, gel-shift assays coupled with random binding site selection did not lead to an enrichment of sequences, even after several rounds of selection. We consider these findings to indicate that when acting alone, the GLK1 protein binds DNA in a non-sequence-specific manner. Therefore, we anticipate that GLK proteins act in concert with partners to attain specificity in DNA binding. Importantly, GLK1 and GLK2 have been shown to interact with two G-box binding factors in yeast (Tamai et al., 2002), and of the 23 ChIP-positive genes identified in this study, eight contain a perfect G-box in the first 500 bp upstream of the annotated transcription start site (see Supplemental Table 9 online). Therefore, it is possible that various combinations of

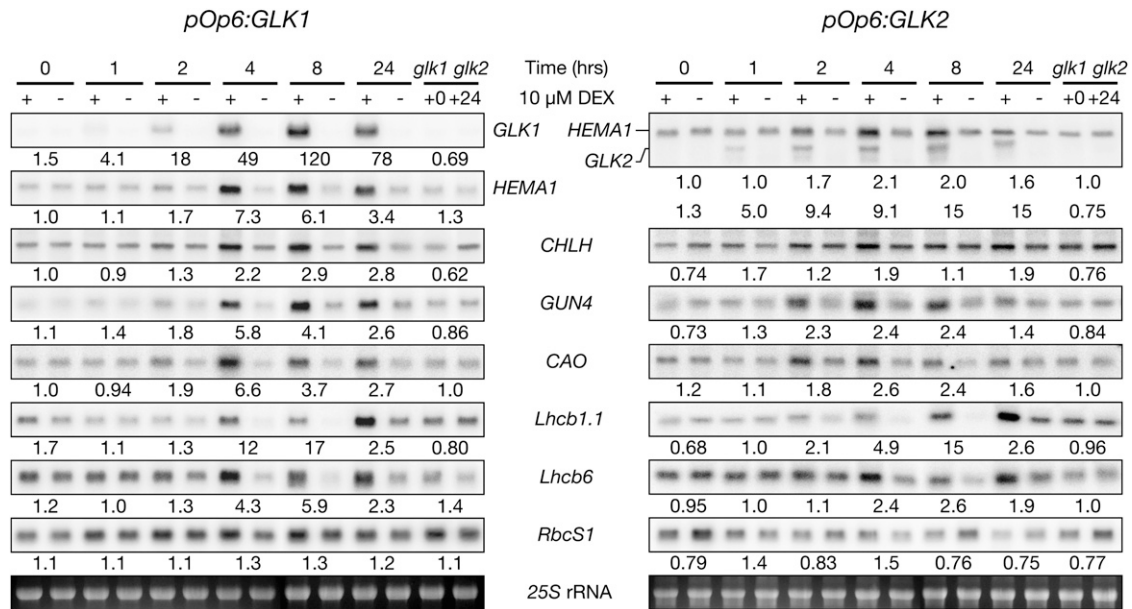


Figure 6. Accumulation of Photosynthesis-Related Transcripts following *GLK* Induction.

RNA gel blot analysis following *GLK* induction. Replicate sets of seedlings carrying either *pOp6:GLK1* or *pOp6:GLK2* were simultaneously treated with 10 μ M DEX (+) or mock-treated with 0.1% DMSO (–) and harvested at the times shown. Seedlings were grown under a 16-h-light/8-h-dark cycle, and induction was performed 6 h after dawn. *glk1 glk2* seedlings carrying the *LhGR-N* transgene were used as negative controls and harvested either immediately after addition of DEX (+0) or 24 h afterwards (+24). Ten micrograms of total RNA was loaded per lane, and replicate blots were probed and quantified using a phosphor imager. Values below each blot represent the fold ratio calculated as (induced value)/(mock value), after standardization to 25S rRNA on the ethidium bromide–stained gel.

transcription factors that recognize distinct *cis*-elements mediate *GLK*-dependent regulation of transcription. Such a scenario would provide a mechanism for integrating developmental and environmental signals.

GLK* Genes Regulate *Lhcb6* Transcription Independently of *phyB

Photosynthetic development is influenced by red light-perceiving phytochromes (*phy*), and *phyB* mutant seedlings are defective in deetiolation and remain pale green throughout development (Reed et al., 1994). To establish whether *phyB* is required for *GLK*-dependent regulation of photosynthesis, we generated a *phyB glk1 glk2* triple mutant. Three-week-old triple mutants exhibit a combination of *glk1 glk2* and *phyB* parental phenotypes: morphologically they resemble *phyB* mutants with elongated petioles and thin leaves, and they contain less chlorophyll than either of the parents (Figures 9A and 9B). This additive effect implies that *phyB* and *GLK* signals act separately during photosynthetic development.

To assess this idea further, etiolated seedlings of each genotype were grown for 16 h under continuous white, red, or blue light, and *Lhcb6* transcript levels were determined as a marker of photosynthetic gene expression patterns. Under white and blue light treatments, *Lhcb6* transcripts were lower in *phyB* than the wild type, but higher than in *glk1 glk2* mutants; notably, the reverse was true for red light (Figure 9C). Significantly, the triple

mutant was indistinguishable from *glk1 glk2* mutants in white and blue light, but accumulated substantially lower levels of *Lhcb6* transcripts in the red light conditions that favor *phyB*-dependent photomorphogenesis. This result suggests that *phyB* does not act exclusively upon *Lhcb6* via *GLK* proteins and suggests a degree of independence between the *phyB* and *GLK* pathways.

***GLK* Transcript Levels Are Regulated by Feedback from the Plastid**

Many genes encoding photosynthetic proteins are regulated in response to retrograde feedback signals from the plastid. One of these signaling pathways is defined by the *genomes uncoupled* (*gun*) mutants, which aberrantly accumulate nuclear photosynthetic gene transcripts in the presence of dysfunctional plastids (Susek et al., 1993). Of the five original *gun* mutants, four are defective in tetrapyrrole synthesis, implying that perturbations in levels of tetrapyrrole intermediates are generally linked with the *GUN* repressive signal from the plastid (Strand et al., 2003). The signal molecule itself is not a tetrapyrrole but may be a reactive oxygen species resulting from free phototoxic tetrapyrroles (Mochizuki et al., 2008; Moulin et al., 2008). Retrograde plastid signaling can be induced in germinating seedlings by adding either norflurazon (NF), which causes photooxidative damage, or lincomycin (L), which inhibits plastid translation. Because of the different signaling mechanisms induced by these inhibitors, responses vary depending on the gene assayed (Gray et al.,

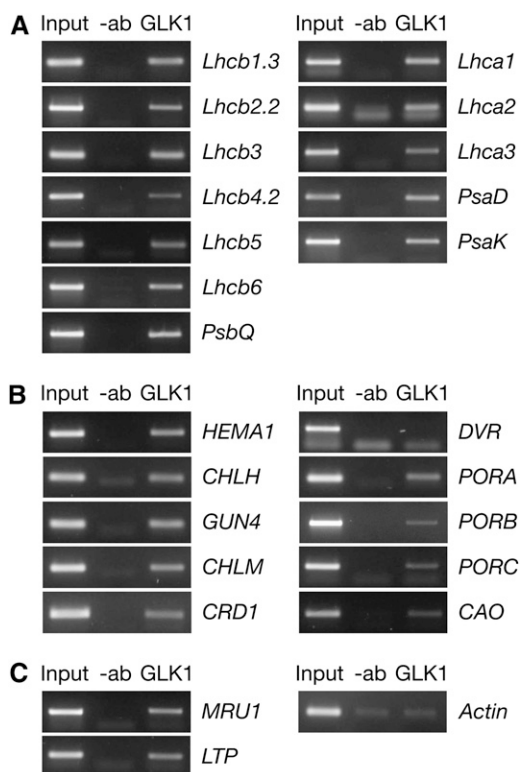


Figure 7. GLK Proteins Bind the Promoter Sequences of Nuclear Photosynthetic Genes.

PCR amplification of promoter sequences following ChIP assays. PSII and PSI genes (**A**), chlorophyll biosynthesis genes (**B**), and an actin negative control and two genes of unknown function, MRU1 (At5g35490) and LTP (At5g48490) (**C**). Sheared chromatin was subjected to immunoprecipitation with GLK1 antibody (+ab) or mock precipitated without antibody (–ab). Genomic DNA was used as a positive control (Input). Association of GLK1 with the promoter of a given gene is determined by enrichment of the PCR product in +ab compared with –ab lanes.

2003). Used in combination with *gun* mutants, NF and L can be used to establish the mechanism by which transcription of a nuclear gene is responsive to plastid retrograde signals.

To determine whether *GLK* genes respond to retrograde signals from the plastid, we measured transcript levels in the wild type, *glk1 glk2*, and *gun1 gun5* double mutants grown in the presence or absence of plastid inhibitors. The *gun1 gun5* double mutant exhibits an enhanced *gun* phenotype compared with the respective single mutants (Mochizuki et al., 2001). To verify that the treatments and genotypes were performing as expected, we monitored transcript levels of *Lhcb6*, *RbcS1*, and *CARBONIC ANHYDRASE1 (CA1)*, all of which are highly sensitive to plastid signals (Strand et al., 2003). Transcript levels of these genes were downregulated in response to NF and L, and this effect was strongly suppressed by the *gun1 gun5* mutations. This suggests that in treated wild-type plants, the GUN signaling pathway mediates the observed response to NF and L (Figure 10).

Interestingly, *GLK1* and *GLK2* were differentially affected by the *gun1 gun5* mutations, even in the absence of plastid inhib-

itors: *GLK1* transcripts accumulated to higher levels in the *gun1 gun5* background than in wild type, whereas the reverse was true for *GLK2*. This observation implies distinct regulation of each gene, a suggestion that is further supported by the differential response of *GLK1* and *GLK2* to NF- and L-mediated plastid damage. While NF and L led to much lower transcript levels of both genes in the wild type, the *gun1 gun5* mutations strongly rescued this effect on *GLK2* but only weakly rescued the effect on *GLK1*. Intriguingly, we found that the transcript size of *GLK1* was consistently reduced in wild-type plants treated with NF and L, whereas the transcript size of *GLK2* and other genes was unaffected (Figure 10). This result has not been observed under any other conditions previously investigated and may indicate some form of posttranscriptional regulation of *GLK1*. Together, these observations imply that both *GLK1* and *GLK2* respond to the developmental status of the chloroplast and that each may be sensitive to different cues.

In monitoring the control genes, we noticed that *Lhcb6*, *RbcS1*, and *CA1* were less responsive to plastid inhibitors in *glk1 glk2* mutants than in the wild type (Figure 10). Specifically, *RbcS1* and *CA1* transcript levels were higher in mutants than in the wild type following L or NF treatment. This result could be

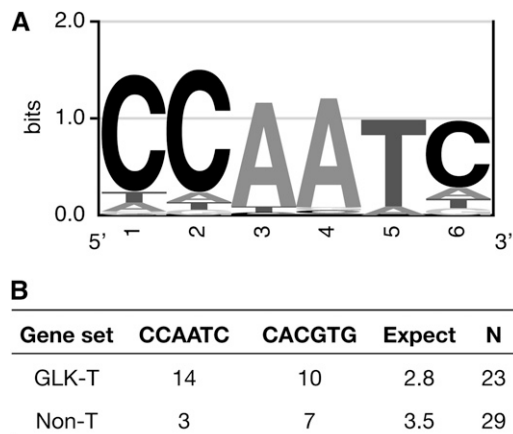


Figure 8. A Putative Promoter Binding Element of GLK Transcription Factors.

(**A**) The first 500 bases upstream of the annotated transcriptional start site of 23 genes identified as positive by ChIP (Figure 7) were analyzed for potential consensus *cis*-elements using Weeder. The highest scoring six-base motif was CCAATC. All of the occurrences of CCAATC with one or fewer substitutions were used to generate a logo of the consensus sequence. The size of the letter at each position is scaled relative to the information content (a measure of conservation), reflecting the frequency of the corresponding base at each position. This logo is energy normalized using relative entropy to compensate for the low GC content in *Arabidopsis*.

(**B**) The upstream 500 bases of the 23 GLK targets (GLK-T) and of 29 photosynthesis-related non-GLK targets (Non-T) were searched for the presence of the CCAATC and CACGTG motifs. The total number of perfect occurrences of each motif over all sequences is given in the table. “Expect” gives the number of expected occurrences of any 6-bp motif over the total sequence length considered, given an equiprobable distribution of nucleotides. Gene lists and a breakdown of element frequencies is provided in Supplemental Table 9 online.

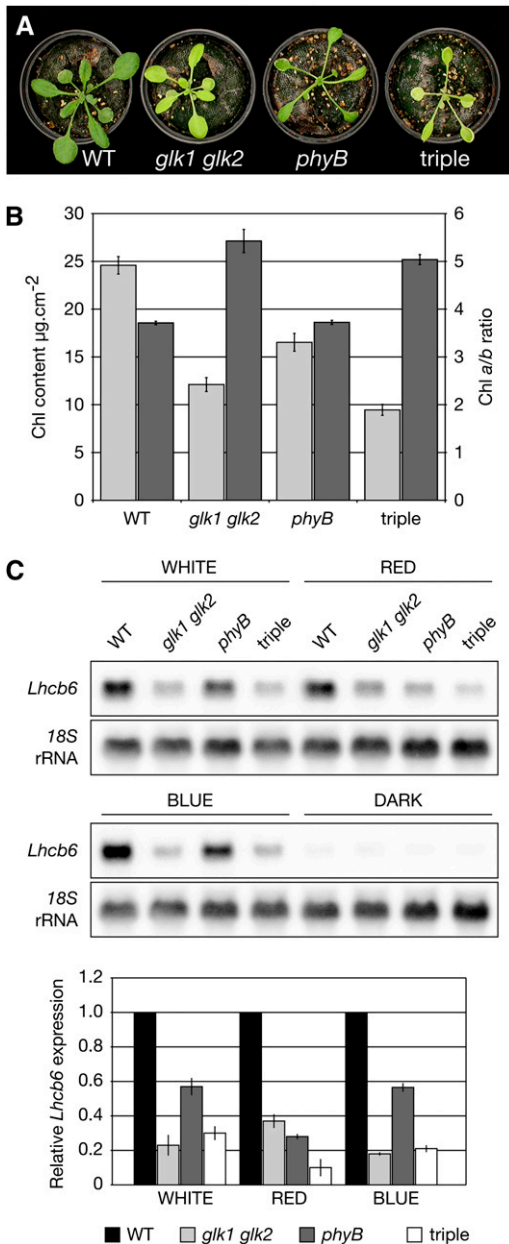


Figure 9. GLK- and phyB-Derived Signals Act Independently upon *Lhcb6* Expression.

(A) Three-week-old, glasshouse-grown plants of the following genotypes (left to right): the wild type, *glk1 glk2*, *phyB*, and *phyB glk1 glk2* (triple).

(B) Total chlorophyll content (light gray) and chlorophyll *a/b* ratio (dark gray) of genotypes shown in **(A)**. Error bars show mean \pm SE ($n = 10$ individual plants).

(C) RNA gel blot analysis showing accumulation of *Lhcb6* transcripts in seedlings of genotypes shown in **(A)**. Etiolated seedlings were exposed to continuous white, red, or blue light or maintained in the dark for 16 h. Ten micrograms of total RNA was loaded per lane, and replicate blots were hybridized with *Lhcb6* or 18S rRNA ³²P-labeled DNA fragments and quantified with a phosphor imager. The chart shows *Lhcb6* transcript levels, relative to 18S rRNA and standardized such that the wild type = 1 in each light treatment. Column heights denote the mean value from

interpreted to suggest that *glk1 glk2* mutants exhibit a weak *gun*-like phenotype. This notion is consistent with the reduced levels of chlorophyll intermediates in *glk1 glk2* mutants, a metabolic state that could perturb the tetrapyrrole pool and thus influence the GUN pathway (Mochizuki et al., 2008; Moulin et al., 2008; von Gromoff et al., 2008).

DISCUSSION

The chloroplast is a metabolically and functionally dynamic organelle. During the day, varying levels of light interception must be carefully balanced with rates of carbon fixation, and at night, photosynthesis halts and the chloroplast mobilizes starch reserves. While many of these changes are mediated by rapid posttranslational control, the circadian rhythm of numerous photosynthesis-related transcripts indicates that transcriptional control in the nucleus is a significant factor. We have shown here that GLK transcription factors help regulate the synchronous transcription of a suite of genes required for the light-dependent steps of photosynthesis, in both the light and the dark. We also show that *GLK* genes themselves respond to retrograde signals from the chloroplast and that at least some of the components of the GLK pathway act independently of the *phyB* signaling pathway. As such, GLK transcription factors act as nuclear regulators of photosynthetic capacity.

A number of transcription factors have previously been reported to coregulate photosynthesis-related genes, but only GLK proteins have been shown to primarily affect such targets. For example, the bZIP protein HY5 acts downstream of the photoreceptors to regulate photomorphogenesis, of which the concerted transcription of photosynthesis-related genes is just one aspect (Oyama et al., 1997). Although genes required for photosynthesis are highly overrepresented among HY5 targets compared with the genome as a whole, the majority of HY5 targets are other transcription factors. This balance reflects the position of HY5 as a high-level regulator of photomorphogenesis (Lee et al., 2007). Moreover, because *hy5* mutants are defective in root growth and hormone response, HY5 must have additional roles beyond photomorphogenesis (Oyama et al., 1997; Cluis et al., 2004). HY5 binding sites, primarily G-box elements, are highly represented in the promoters of other transcription factors, including *GLK2*, but intriguingly not *GLK1* (Lee et al., 2007).

Of the two, *GLK2* is much more responsive to early light induction in a phy-dependent manner (Tepperman et al., 2006). Since HY5 acts downstream of *phy*, it seems reasonable to suppose that HY5 activates *GLK2* and, furthermore, that GLK transcription factors regulate a more specific subset of genes than early components of the classical photomorphogenesis pathway. Another example of G-box binding transcription factors that coordinate photosynthetic gene expression is the phytochrome interacting factor (PIF) family (Castillon et al., 2007). PIF3 regulates a large number of genes during photomorphogenesis, including *CHLH* and *CAO* (Monte et al., 2004),

two experimental replicates, with the error bars showing the maximum and minimum values obtained across both replicates.

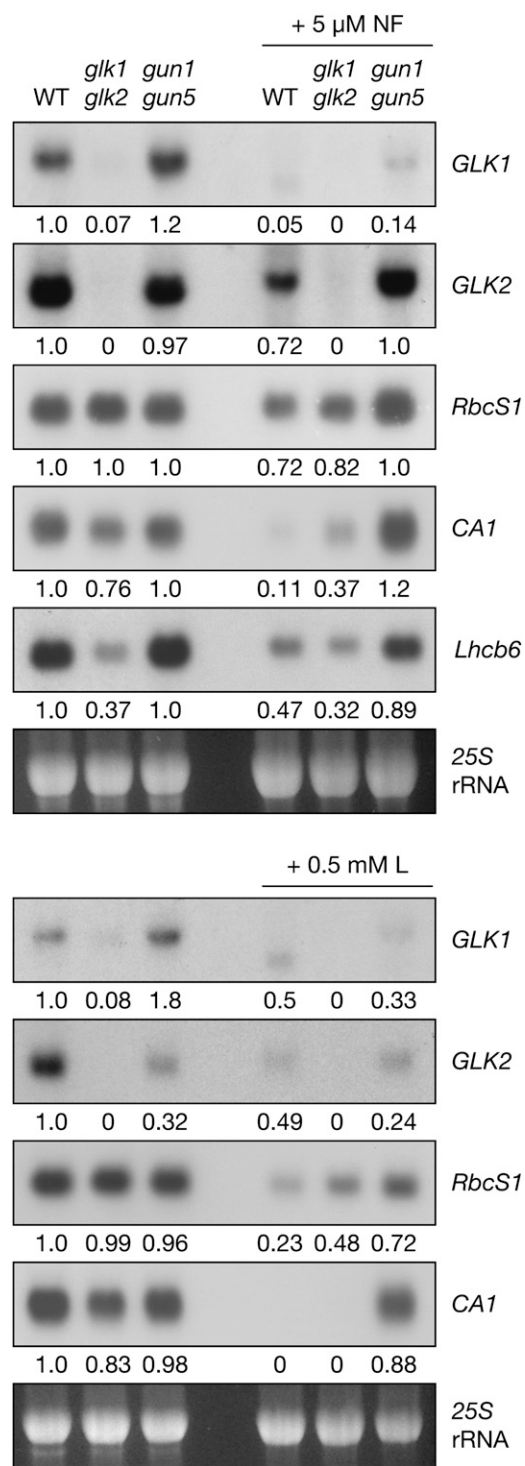


Figure 10. GLK Transcript Levels Are Sensitive to Plastid-Derived Retrograde Signals.

RNA gel blot analysis showing accumulation of *GLK1*, *GLK2*, *RbcS1*, *CA1*, and *Lhcb6* transcripts in response to inhibitor-induced plastid damage. Surface-sterilized seeds were sown on media supplemented with 5 μ M NF (top panel) or 0.5 mM L (bottom panels). Ten micrograms of total RNA was loaded per lane, and replicate blots were hybridized with

whereas the direct binding of PIF1 is limited to a G-box in the *PORC* promoter (Moon et al., 2008). Whether GLK proteins work in conjunction with these other transcription factors remains to be established, but given that GLK proteins can interact with G-box binding factors (Tamai et al., 2002), it is unlikely that they act in isolation.

Our results conflict with a recent assessment of the GLK1 regulon, which consisted of a microarray analysis of a GLK1-overexpressing line in a wild-type background (Savitch et al., 2007). The authors reported that GLK1 overexpression induced the expression of a variety of disease- and defense-related genes but had no effect on photosynthesis-related genes. We believe this discrepancy to be the result of three factors. First, expression in a wild-type background would reduce the sensitivity of the experiment in that the plants are already photosynthetically competent. Second, strong constitutive GLK expression leads to pleiotropic effects, such as delayed flowering, leaf epinasty, and increased anthocyanin accumulation, the latter of which may be indicative of stress (Waters et al., 2008; data not shown). Third, constitutive gene expression confounds primary and secondary effects, a situation that was overcome in our study using an inducible expression approach. It is noteworthy, however, that Savitch et al. (2007) reported significant upregulation of *MRU1* and *LTP*, consistent with our findings.

Primary versus Secondary Effects of GLK Action

The use of an inducible gene expression system circumvented many problems associated with direct transcriptome comparisons between genotypes as a means for determining *GLK* function. Nevertheless, a 4-h induction time conceivably is sufficient for events downstream of immediate *GLK* activity to become apparent. CHIP assays confirmed that *GLK1* protein is associated with the promoters of the most significantly affected genes following *GLK* induction, implying that such genes are likely to be primary targets. Accordingly, we infer that affected genes whose promoters do not interact with *GLK1* (such as *COR15a*) are indirect, secondary targets of *GLK* genes. Notably, although a clear aspect of the *glk1 glk2* mutant phenotype is the decreased abundance of thylakoid membranes and grana, none of the known components of the thylakoid biogenesis machinery, such as *FZL* (Gao et al., 2006) or *VIPP1* (Kroll et al., 2001; Aseeva et al., 2007), were activated by *GLK* expression. This implies that reduced thylakoid abundance in *glk1 glk2* mutants is a secondary effect of reduced LHC and chlorophyll levels.

One model for the formation of granal thylakoids suggests that attractive forces between LHCII trimers on closely appressed thylakoids cause membrane adhesion (Allen and Forsberg, 2001; Standfuss et al., 2005). Another suggestion is that the crystalline arrays of PSII complexes that form on thylakoid membranes

³²P-labeled DNA fragments. Blots were visualized by autoradiography and quantified by densitometry. Values below each blot denote the fold-change relative to the wild type grown without inhibitors, standardized to 25S rRNA on the ethidium bromide-stained gel. This experiment was performed twice with similar results.

when LHC is bound may assist the assembly of grana (Kovacs et al., 2006). Support for a mechanistic role for LHC and chlorophyll in grana formation is provided by the rice (*Oryza sativa*) mutant *non-yellow coloring1* (*nyc1*). During senescence, LHCII and chlorophyll are selectively retained in *nyc1*, and the mutant also maintains thylakoid membranes with a high degree of grana stacking (Kusaba et al., 2007). *NYC1* encodes a putative chlorophyll *b* reductase enzyme responsible for the early stages of chlorophyll *b* degradation. It is thus likely that retention of LHCII in the *nyc1* mutant is a consequence of LHCII stabilization by chlorophyll *b* (Kusaba et al., 2007) and that grana are maintained in senescent leaves as a result of that stabilization. Accordingly, by coordinating expression of *Lhc* and chlorophyll biosynthesis genes, *GLK* transcription factors promote the formation of stable LHCII-PSII supercomplexes and, hence, the formation of grana.

GLK genes strongly upregulate components of the chlorophyll pathway, in particular *HEMA1*, *CHLH*, *CRD1*, and *CAO* (Figure 4). Transcriptional profiles of the entire metabolic pathway in *Arabidopsis* revealed that these four genes are tightly coregulated: they are strongly and synchronously induced during photomorphogenesis, and they cycle in-phase with one another, and with *Lhcb1*, under circadian control (Matsumoto et al., 2004). Notably, while much of the fine-tuning of tetrapyrrole biosynthesis is performed by posttranslational mechanisms (Tanaka and Tanaka, 2007), these four key genes are under transcriptional regulation, and *GLK* genes are at least partially responsible for this process.

GLK genes also promote the expression of all three *POR* genes. However, interpreting the impact of this role is difficult because different *POR* gene expression profiles have been reported in the literature. For example, one report suggested that both *PORA* and *PORB* are active in dark-grown seedlings, but *PORA* is rapidly repressed upon light exposure and only *PORB* remains active (Armstrong et al., 1995). However, Matsumoto et al. (2004) reported that both *PORA* and *PORB* levels decline rapidly after the onset of light, yet both are active and under circadian control in mature plants. *PORC*, meanwhile, is induced by light along with the majority of the tetrapyrrole enzymes (Matsumoto et al., 2004) and is thought to have an active role in mature leaves together with *PORB* (Frick et al., 2003). Regardless of the precise expression patterns of *POR* genes, coordinated induction by *GLK* genes implies that all three share a common regulatory element and demonstrates that *GLK* transcription factors regulate much of the chlorophyll pathway in both the dark and the light.

GLK Targets beyond Chlorophyll and Light Harvesting

While 13 of the 20 genes listed in Table 1 are chloroplast localized, several have unknown function and ambiguous location but are predicted to be *GLK1* targets based on ChIP data (Figure 7). For example, *MRU1* is strongly induced and encodes a 58-amino acid protein with no recognized functional domains (Goto and Naito, 2002). WoLF PSORT weakly predicts that *MRU1* is targeted to the mitochondrion, followed by equal probability of being targeted to the chloroplast, cytosol, or peroxisome. Similarly, the lipid transfer protein (*LTP*) encoded

by At5g48490 putatively functions in lipid binding and transport (Lascombe et al., 2008), which may reflect a requirement for thylakoid lipids. The increased expression of *COR15a* and a thylakoid lumen-resident rhodanese-like domain-containing protein (At2g42220) following *GLK* induction is particularly intriguing. *COR15a* is a cold-induced stromal protein that increases tolerance to freezing temperatures by protecting stromal enzymes from frost damage (Nakayama et al., 2007).

The link to photosynthesis in nonacclimated plants is unclear. However, decreased *COR15a* protein and transcript levels are observed in mutants with impaired chloroplast development (Nakayama et al., 2007), and levels are downregulated sixfold in a chlorophyll biosynthetic mutant lacking Mg-Proto methyltransferase (Pontier et al., 2007). These findings suggest that expression of *COR15a* is responsive to broad changes in chloroplast composition and supports our supposition that *COR15a* is an indirect target of *GLK* proteins. Rhodanases, meanwhile, have unknown biological functions in plants, but they catalyze the transfer of sulfur atoms to nucleophilic acceptors, and at least one rhodanese is located in the thylakoids (Bauer et al., 2004). It is conceivable that rhodanese-like proteins may be required for the repair or synthesis of iron-sulfur clusters, such as those found in PSI and in the Rieske protein of the cytochrome *b6/f* complex (Balk and Lobrèaux, 2005). Given the role of *GLK* genes in contributing to photosystem assembly, characterization of these rhodanases may provide insight into how *GLK* proteins ensure that photosynthetic capacity is optimized in different environmental and developmental conditions.

GLK Function in the Context of Whole-Plant Physiology

Within a plant, leaves are developmentally heterogeneous and are exposed to different light regimes. Shaded leaves, for example, are thinner than leaves exposed to frequent full sun, and shaded chloroplasts contain more chlorophyll *b* and grana to optimize light harvesting (Anderson et al., 1995; Weston et al., 2000). Such long-term developmental variation implies regulation of photosynthesis at a transcriptional level. Notably, *GLK*-overexpressing plants accumulate more chlorophyll and chlorophyll-related/*Lhc* transcripts than the wild type, while *RbcS* transcripts remain unchanged: this implies a distinct regulation of the balance between the light-dependent steps of photosynthesis and carbon fixation. Such shifts in balance are observed in *Arabidopsis* acclimating to a transition from high to low light intensity, when light becomes limiting for photosynthesis (Walters and Horton, 1994).

Thus, the *GLK* overexpression phenotype may be interpreted as mimicking a response to limiting light and hints at an adaptive function for *GLK* genes. The photosynthetic apparatus responds to changes in light intensity and quality mainly through shifts in the redox balance in the chloroplast (Walters, 2005; Pfannschmidt et al., 2009). A redox-sensitive kinase, such as STN7, is certainly responsible for short-term acclimation through state transitions (Bellafiore et al., 2005) and may also be a candidate for signaling to the nucleus for long-term transcriptional changes that regulate photosystem stoichiometry (Bonardi et al., 2005).

Data presented here suggest that long-term developmental responses to light intensity are not wholly *GLK* dependent (Figure

1). This observation suggests that while GLK proteins are required for absolute levels of nuclear photosynthetic gene expression, they operate alongside additional regulatory factors that mediate redox signaling. It remains to be established whether *GLK* genes themselves respond to changes in photosynthetic conditions. Given that *GLK* genes are sensitive to feedback signaling from the chloroplast (Figure 10), they may operate downstream of plastid retrograde signaling to form part of a more long-term acclimatory response.

The fact that various photoreceptor mutants acclimate normally (Walters et al., 1999) shows that redox signaling rather than photoreceptor signaling mediates changes in photosystem stoichiometry. Nevertheless, both red and blue photoreceptors are required for normal chloroplast biogenesis, especially during deetiolation (Sullivan and Deng, 2003). If *GLK* and *phyB* operated in the same direct pathway, we would expect to observe an epistatic relationship in the triple mutant. The additive phenotype of the triple mutant may result from *phyB* acting partly through GLKs and partly through other factors, while GLKs are responsive to *phyB* and other regulators (e.g., *phyA*). This is consistent with the well-characterized PIF-dependent pathways and microarray studies showing that both *phyA* and *phyB* regulate *GLK* transcription (Tepperman et al., 2006). Furthermore, photosynthetic gene expression is especially compromised in *glk1 glk2* mutants in blue light, which suggests that cryptochromes also regulate *GLK* activity and is consistent with the role of cryptochromes in regulating chlorophyll biosynthesis (Stephenson and Terry, 2008). Experiments to investigate these interactions more precisely are underway. However, it is notable that *GLK2*, but not *GLK1*, is strongly induced in etiolated seedlings exposed to 45 min of blue light (AtGenExpress light data set, available at <http://www.Arabidopsis.org>).

The microarray data presented here and previous work (Waters et al., 2008) have shown that the two GLK proteins are functionally equivalent. However, results shown here (Figure 10) and elsewhere (Tepperman et al., 2006) suggest that *GLK1* and *GLK2* are differentially regulated at the transcriptional level. While the proteins may be capable of performing similar functions, differential transcription may explain the existence of a duplicated gene pair, with one being coexpressed with additional genes to perform a specific function. Recently, *GLK1* was implicated as a central component in the signaling network for organic nitrogen metabolism (Gutiérrez et al., 2008), and *GLK1* was predicted to promote expression of a cytosolic Gln synthetase, At3g17820. Although we detected no significant change in expression of this gene in our experiments, it is quite conceivable that organic nitrogen status would influence photosynthetic gene expression. Therefore, the possibility that *GLK* genes respond to organic nitrogen as a regulatory input should be considered further. Additional roles for individual GLK proteins may emerge through similar studies of systems biology.

METHODS

Plant Material and Growth Conditions

Arabidopsis thaliana ecotype Columbia-0 was used in all experiments. The *glk1 glk2* mutant as previously described (Fitter et al., 2002) is

available from the European Arabidopsis Stock Centre (NASC ID N9807). *35S:GLK1* and *35S:GLK2* plants were described previously (Waters et al., 2008). The *phyB glk1 glk2* triple mutant was generated by crossing *glk1 glk2* with *phyB-9*, a null allele containing a G-to-A transition that introduces a premature stop codon at amino acid position 397. The allele was originally described as *hy3-EMS142* (Reed et al., 1994). The *gun1 gun5* double mutant has been described previously (Mochizuki et al., 2001). All seeds were imbibed and stratified for 3 d in the dark at 4°C. Seeds were sown on peat-based compost and transferred to individual 42-mm peat plugs (Jiffy Products International). Plants were grown under a 16-h-light and 8-h-dark photoperiod in the greenhouse at 20 to 25°C with supplementary lighting. For controlled growth conditions (data for Figure 1), plants were grown in a Fitotron PG1400.

The activator line LhGR-N(4c), carrying a single copy of the *35S:LhGR-N* construct (Craft et al., 2005), was crossed with the *glk1 glk2* mutant. The dark-green F1 progeny were selected on kanamycin and selfed. The F2 generation was screened for pale green individuals representing *glk1 glk2* homozygotes. These individuals were selfed, and F3 seed was then sown on kanamycin to identify lines homozygous for *35S:LhGR-N*. Seedlings homozygous for *glk1*, *glk2*, and *35S:LhGR-N* were transformed by the floral dip method (Clough and Bent, 1998). Details of vector construction are given in the Supplemental Methods online. Transgenic plants resistant to hygromycin were selected on 1× Murashige and Skoog (MS) salts with 1× Gamborg's vitamins, 20 μg/mL hygromycin B, and 0.8% (w/v) agar. Plants were grown at 20°C under white light (85 μmol quanta·m⁻²·s⁻¹) from fluorescent bulbs.

Light and Plastid Inhibitor Treatments

Surface-sterilized seeds were sown on 1× MS salts, 1× Gamborg's vitamins, and 0.8% (w/v) agar and wrapped in foil before stratification in the dark for 3 d at 4°C. Germination was stimulated by a 2-h exposure to white light, and the seeds were then double-wrapped in foil and moved to a growth room at 20°C for a further 48 h. After this time, seedlings were exposed to 16 h of continuous light. Red and blue light was supplied by an array of Luxeon III StarHex LEDs (Philips Lumileds) mounted in a temperature-controlled incubator maintained at 20°C and installed in a dark room. Both red and blue light were delivered at 20 μmol quanta·m⁻²·s⁻¹, with peak output at 627 and 455 nm respectively, as defined by the manufacturer. For this experiment (Figure 9), white light was supplied by fluorescent tubes at 40 μmol quanta·m⁻²·s⁻¹. Tissue was harvested either in the dark or under the specific light conditions used for growth, as appropriate. For treatment of seedlings with plastid inhibitors (Figure 10), seeds were grown in the same manner except that the media was supplemented with 1% (w/v) sucrose. When the foil was removed, the seedlings were exposed to white light (60 μmol quanta·m⁻²·s⁻¹) with a 16-h-light/8-h-dark cycle for two complete cycles. Tissue was harvested at the beginning of the third cycle.

Growth of Seedlings for Microarray Induction Experiments

Full details are given in the Supplemental Methods online. Briefly, seeds were surface sterilized, resuspended in sterile 0.1% (w/v) agar, and transferred by pipette onto 10-cm square plates containing 1× MS salts, 1× Gamborg's vitamins, 20 μg/mL hygromycin B, and 0.8% (w/v) agar. Excess water was allowed to evaporate, and the seeds were stratified.

After 10 d of growth under a 16-h-light/8-h-dark cycle, ~100 seedlings of equivalent developmental stage were transferred from the plates into 100 mL liquid MS medium in a 250-mL conical flask. The flasks were shaken under the same growth conditions as before. After 48 h of growth in liquid culture, the seedlings were treated with either 10 μM DEX or with 0.1% DMSO (mock induction) and then returned to the same growth conditions. Once the relevant time period had elapsed, seedlings were harvested and flash-frozen in liquid nitrogen.

Microarray Experiments and Data Analysis

Seedlings carrying either *pOp6:GLK1* or *pOp6:GLK2* constructs were grown and treated as described above. For each construct, seedlings were transferred into two separate liquid cultures, which were grown in parallel and treated identically except that one flask was treated with DEX and one mock-treated with DMSO. Each pair of flasks representing an independent biological replicate (four per construct) was grown and treated on different days to control for unintentional day-to-day experimental bias. Treatment was performed 6 h after subjective dawn on each experimental occasion. Details of microarray hybridizations and data analysis are in the Supplemental Methods online.

RNA Analysis

All RNA was isolated by guanidinium thiocyanate–phenol–chloroform extraction (Chomczynski and Sacchi, 2006), except for the data shown in Figure 9, for which a method more suitable for young *Arabidopsis* seedlings was employed (McCormac et al., 2001). For microarray analysis, RNA was further purified with an RNeasy plant RNA extraction kit (Qiagen). RNA gel blots were prepared and hybridized in 0.45 M NaCl at 65°C using ³²P-labeled DNA fragments as described previously (Langdale et al., 1988). RNA gel blots were quantified using a Bio-Rad FX molecular imager and the supplied Quantity One software. Band intensity was determined using the peak count after background subtraction and was normalized to either the 18S rRNA peak count following hybridization or 25S rRNA band on an ethidium bromide–stained gel. Such bands were quantified using a Kodak EDAS-290 camera with the 1D Image Analysis software (Eastman Kodak). The band with the most intense signal was assigned a value of 1, and the hybridization values were standardized accordingly. DNA probes are detailed in the Supplemental Methods online.

ChIP Assays

ChIP assays were performed as described previously (Saleh et al., 2008) with modifications. Formaldehyde cross-linked chromatin complexes were extracted from 3-week-old 35S:*GLK1* plants and sheared to small fragments of ~500 bp (200 to 1000 bp) by sonication. Antibody against *Arabidopsis* GLK1 (see Supplemental Methods online for purification procedure) and salmon sperm DNA/protein A agarose beads (Upstate) were used for immunoprecipitation. The coprecipitated DNA was eluted, reverse cross-linked, purified, and finally amplified using primers specific to the promoter regions of the candidate genes. Sequences of PCR primers, which amplify fragments within 500 bp of the ATG in each case, are provided in Supplemental Table 8 online.

Analysis of Chlorophyll Precursors

Approximately 80 mg of dry *Arabidopsis* seed was surface sterilized and sown on MS plates containing 0.8% (w/v) agar. Using equal amounts of seed, each genotype was considered the most appropriate standardization method, since the hypocotyl and root contribute more to the seedling mass than the cotyledons in the dark, and differences in growth rates may skew the data if measured on a per-weight basis. Following pretreatment of 2 d at 4°C in the dark and 8 h in the light at 24°C, seedlings were grown in the dark at 24°C for 4 d, after which ALA or DP feeding solution (10 mM ALA or DP in 5 mM MgCl₂ and 10 mM HEPES, pH 7.0) was added to each plate. The seedlings were further incubated overnight and harvested under dim green light. Chlorophyll precursors were extracted from etiolated seedlings with *N,N*-dimethylformamide for 12 h at 4°C in darkness, as described previously (Moran and Porath, 1980). The supernatant was collected by centrifugation for 5 min at 13,000g. Fluorescence emission spectra were recorded from 560 to 700 nm using an LS50

luminescence spectrophotometer (Perkin-Elmer) at room temperature. The samples were excited at 440, 420, and 400 nm for detection of Pchl_{ide}, MgProtoIX/MgProtoIX ME, and Proto IX, respectively.

Transmission Electron Microscopy

Seedlings were grown *in vitro* as for analysis of chlorophyll precursors. After 4 d of growth in the dark, whole seedlings were fixed in the dark by immersion in ice-cold fixative comprised of 4% paraformaldehyde and 3% glutaraldehyde in 0.05 M potassium phosphate buffer, pH 7, followed by vacuum infiltration. The samples were maintained in the dark and at 4°C overnight, and then the cotyledons were dissected out. Subsequent steps were performed as described previously (Waters et al., 2008). A total of 15 sections were taken from three individual seedlings of each genotype. Twelve of these sections were then used to calculate prolamellar body size, taking one measurement from each section.

Promoter Sequence Analysis

Promoter sequences for each gene were downloaded in FASTA format from The Arabidopsis Information Resource (TAIR). Calvin cycle genes were identified using the AraCyc tool (TAIR) and further sorted by removing duplicate loci. Genes encoding chloroplast-specific enzymes were distinguished using TargetP (Emanuelsson et al., 2007), and other genes were discarded. Sequences were analyzed using a local installation of the Weeder program (available at <http://159.149.109.9/modtools/>), searching for 6-, 8-, and 10-bp motifs in the forward strand only. To obtain a significance value, the score for each evaluated motif was submitted into the P value calculator tool available at the same website. The occurrence of motifs in each promoter was calculated using the Locator program provided with Weeder, using a threshold of one substitution allowable per motif. The motif consensus logo was generated using EnoLOGOS (Workman et al., 2005).

Accession Numbers

MIAME-compliant data from microarray experiments were deposited with ArrayExpress (www.ebi.ac.uk/microarray-as/ae/) under accession number E-MEXP-1794. Sequence data for *GLK1* and *GLK2* can be found in the GenBank/EMBL or Arabidopsis Genome Initiative databases under the following accession numbers: *GLK1*, 816579 (At2g20570) and *GLK2*, 834442 (At5g44190). Accession numbers for other genes used in the study are listed in Supplemental Table 10 online.

Author Contributions

M.T.W. did the majority of the experimental work, contributed to project design, and wrote the article. P.W. did the chlorophyll precursor assays and the ChIP experiments. M.K. and R.G.C. provided technical assistance with the array experiments. N.J.S. designed the array experiments and data analysis. J.A.L. designed and supervised the overall project, provided the funding, and wrote the article.

Supplemental Data

The following materials are available in the online version of this article.

Supplemental Figure 1. Spectrofluorometric Analysis of Chlorophyll Precursors.

Supplemental Figure 2. Phenotypic Rescue of *glk1 glk2* by *pOp6:GLK1* and *pOp6:GLK2*.

Supplemental Figure 3. Phenotypic Rescue of *glk1 glk2* by 35S:*GLK1-FLAG* and 35S:*GLK2-FLAG*.

Supplemental Figure 4. Induction of *GLK1* and *GLK2* Transcripts from the *pOp6* Promoter.

Supplemental Figure 5. Overexpression of Individual Photosynthetic Genes Does Not Rescue *glk1 glk2*.

Supplemental Table 1. All Genes That Pass Significance Criteria following Induction of *GLK1*.

Supplemental Table 2. All Genes That Pass Significance Criteria following Induction of *GLK2*.

Supplemental Table 3. All Upregulated Genes That Pass Significance Criteria in Combined Data Set following Induction of *GLK1* and *GLK2*.

Supplemental Table 4. All Downregulated Genes That Pass Significance Criteria following Induction of *GLK1*.

Supplemental Table 5. All Downregulated Genes That Pass Significance Criteria following Induction of *GLK2*.

Supplemental Table 6. Changes in Genes Encoding Steps of the Chlorophyll Biosynthetic Pathway.

Supplemental Table 7. Changes in Genes Encoding Subunits of Photosystems I and II.

Supplemental Table 8. Primers Used in Chromatin Immunoprecipitation Experiments.

Supplemental Table 9. Motif Instances in GLK Targets and Non-GLK Targets.

Supplemental Table 10. Accession Numbers for Sequence Data.

Supplemental Methods.

ACKNOWLEDGMENTS

We thank Jayne Davis and Julie Bull for technical assistance and members of the Langdale lab for discussions throughout the course of the work. We also thank three anonymous reviewers for helpful suggestions. This work was funded by grants from the Biotechnology and Biological Science Research Council and the Gatsby Charitable Foundation to J.A.L.

Received December 17, 2008; revised March 20, 2009; accepted April 3, 2009; published April 17, 2009.

REFERENCES

- Allen, J.F., and Forsberg, J. (2001). Molecular recognition in thylakoid structure and function. *Trends Plant Sci.* **6**: 317–326.
- Anderson, J.M., Chow, W.S., and Park, Y.-I. (1995). The grand design of photosynthesis: Acclimation of the photosynthetic apparatus to environmental cues. *Photosynth. Res.* **46**: 129–139.
- Armstrong, G.A., Runge, S., Frick, G., Sperling, U., and Apel, K. (1995). Identification of NADPH:protochlorophyllide oxidoreductases A and B: A branched pathway for light-dependent chlorophyll biosynthesis in *Arabidopsis thaliana*. *Plant Physiol.* **108**: 1505–1517.
- Aseeva, E., Ossenbühl, F., Sippel, C., Cho, W.K., Stein, B., Eichacker, L.A., Meurer, J., Wanner, G., Westhoff, P., Soll, J., and Vothknecht, U.C. (2007). *Vipp1* is required for basic thylakoid membrane formation but not for the assembly of thylakoid protein complexes. *Plant Physiol. Biochem.* **45**: 119–128.
- Balk, J., and Lobrèaux, S. (2005). Biogenesis of iron-sulfur proteins in plants. *Trends Plant Sci.* **10**: 324–331.
- Bauer, M., Dietrich, C., Nowak, K., Sierralta, W.D., and Papenbrock, J. (2004). Intracellular localization of *Arabidopsis* sulfurtransferases. *Plant Physiol.* **135**: 916–926.
- Bellaïfiore, S., Barneche, F., Peltier, G., and Rochaix, J.-D. (2005). State transitions and light adaptation require chloroplast thylakoid protein kinase STN7. *Nature* **433**: 892–895.
- Bonardi, V., Pesaresi, P., Becker, T., Schleiff, E., Wagner, R., Pfannschmidt, T., Jahns, P., and Leister, D. (2005). Photosystem II core phosphorylation and photosynthetic acclimation require two different protein kinases. *Nature* **437**: 1179–1182.
- Castillon, A., Shen, H., and Huq, E. (2007). Phytochrome interacting factors: Central players in phytochrome-mediated light signaling networks. *Trends Plant Sci.* **12**: 514–521.
- Chomczynski, P., and Sacchi, N. (2006). The single-step method of RNA isolation by acid guanidinium thiocyanate-phenol-chloroform extraction: Twenty-something years on. *Nat. Protocols* **1**: 581–585.
- Clough, S.J., and Bent, A.F. (1998). Floral dip: a simplified method for *Agrobacterium*-mediate transformation of *Arabidopsis thaliana*. *Plant J.* **16**: 735–743.
- Cluis, C.P., Mouchel, C.F., and Hardtke, C.S. (2004). The *Arabidopsis* transcription factor HY5 integrates light and hormone signaling pathways. *Plant J.* **38**: 332–347.
- Craft, J., Samalova, M., Baroux, C., Townley, H., Martinez, A., Jepson, I., Tsiantis, M., and Moore, I. (2005). New pOp/LhG4 vectors for stringent glucocorticoid-dependent transgene expression in *Arabidopsis*. *Plant J.* **41**: 899–918.
- Emanuelsson, O., Brunak, S., von Heijne, G., and Nielsen, H. (2007). Locating proteins in the cell using TargetP, SignalP, and related tools. *Nat. Protoc.* **2**: 953–971.
- Espineda, C.E., Linford, A.S., Devine, D., and Brusslan, J.A. (1999). The AtCAO gene, encoding chlorophyll a oxygenase, is required for chlorophyll b synthesis in *Arabidopsis thaliana*. *Proc. Natl. Acad. Sci. USA* **96**: 10507–10511.
- Fitter, D.W., Martin, D.J., Copley, M.J., Scotland, R.W., and Langdale, J.A. (2002). GLK gene pairs regulate chloroplast development in diverse plant species. *Plant J.* **31**: 713–727.
- Frick, G., Su, Q., Apel, K., and Armstrong, G.A. (2003). An *Arabidopsis* porB porC double mutant lacking light-dependent NADPH:protochlorophyllide oxidoreductases B and C is highly chlorophyll-deficient and developmentally arrested. *Plant J.* **35**: 141–153.
- Gao, H., Sage, T.L., and Osteryoung, K.W. (2006). FZL, an FZO-like protein in plants, is a determinant of thylakoid and chloroplast morphology. *Proc. Natl. Acad. Sci. USA* **103**: 6759–6764.
- Goslings, D., Meskauskiene, R., Kim, C., Lee, K.P., Nater, M., and Apel, K. (2004). Concurrent interactions of heme and FLU with Glu tRNA reductase (HEMA1), the target of metabolic feedback inhibition of tetrapyrrole biosynthesis, in dark- and light-grown *Arabidopsis* plants. *Plant J.* **40**: 957–967.
- Goto, D.B., and Naito, S. (2002). AtMRD1 and AtMRU1, two novel genes with altered mRNA levels in the methionine over-accumulating mto1-1 mutant of *Arabidopsis thaliana*. *Plant Cell Physiol.* **43**: 923–931.
- Gray, J.C., Sullivan, J.A., Wang, J.-H., Jerome, C.A., and MacLean, D. (2003). Coordination of plastid and nuclear gene expression. *Philos. Trans. R. Soc. Lond. B Biol. Sci.* **358**: 135–145.
- Green, B.R., and Durnford, D.G. (1996). The chlorophyll-carotenoid proteins of oxygenic photosynthesis. *Annu. Rev. Plant Physiol. Plant Mol. Biol.* **47**: 685–714.
- Gutiérrez, R.A., Stokes, T.L., Thum, K., Xu, X., Obertello, M., Katari, M.S., Tanurdzic, M., Dean, A., Nero, D.C., McClung, C.R., and Coruzzi, G.M. (2008). Systems approach identifies an organic nitrogen-responsive gene network that is regulated by the master clock control gene CCA1. *Proc. Natl. Acad. Sci. USA* **105**: 4939–4944.
- Haldrup, A., Lunde, C., and Scheller, H.V. (2003). *Arabidopsis thaliana* plants lacking the PSI-D subunit of photosystem I suffer severe photoinhibition, have unstable photosystem I complexes, and altered

- redox homeostasis in the chloroplast stroma. *J. Biol. Chem.* **278**: 33276–33283.
- Hanaoka, M., Kanamaru, K., Takahashi, H., and Tanaka, K.** (2003). Molecular genetic analysis of chloroplast gene promoters dependent on SIG2, a nucleus-encoded sigma factor for the plastid-encoded RNA polymerase, in *Arabidopsis thaliana*. *Nucleic Acids Res.* **31**: 7090–7098.
- Horton, P., Park, K.-J., Obayashi, T., Fujita, N., Harada, H., Adams-Collier, C.J., and Nakai, K.** (2007). WoLF PSORT: Protein localization predictor. *Nucleic Acids Res.* **35**: W585–587.
- Hosack, D., Dennis, G., Sherman, B., Lane, H., and Lempicki, R.** (2003). Identifying biological themes within lists of genes with EASE. *Genome Biol.* **4**: R70.
- Huang, D., Sherman, B., Tan, Q., Collins, J., Alvord, W.G., Roayaei, J., Stephens, R., Baseler, M., Lane, H.C., and Lempicki, R.** (2007). The DAVID Gene Functional Classification Tool: A novel biological module-centric algorithm to functionally analyze large gene lists. *Genome Biol.* **8**: R183.
- Jansson, S.** (1999). A guide to the Lhc genes and their relatives in *Arabidopsis*. *Trends Plant Sci.* **4**: 236–240.
- Jensen, P.E., Gilpin, M., Knoetzel, J., and Scheller, H.V.** (2000). The PSI-K subunit of photosystem I is involved in the interaction between light-harvesting complex I and the photosystem I reaction center core. *J. Biol. Chem.* **275**: 24701–24708.
- Kannangara, R., Branigan, C., Liu, Y., Penfield, T., Rao, V., Mouille, G., Hofte, H., Pauly, M., Riechmann, J.L., and Broun, P.** (2007). The transcription factor WIN1/SHN1 regulates cutin biosynthesis in *Arabidopsis thaliana*. *Plant Cell* **19**: 1278–1294.
- Klimmek, F., Sjödin, A., Noutsos, C., Leister, D., and Jansson, S.** (2006). Abundantly and rarely expressed Lhc protein genes exhibit distinct regulation patterns in plants. *Plant Physiol.* **140**: 793–804.
- Kovacs, L., Damkjaer, J., Kereiche, S., Illoaia, C., Ruban, A.V., Boekema, E.J., Jansson, S., and Horton, P.** (2006). Lack of the light-harvesting complex CP24 affects the structure and function of the grana membranes of higher plant chloroplasts. *Plant Cell* **18**: 3106–3120.
- Kroll, D., Meierhoff, K., Bechtold, N., Kinoshita, M., Westphal, S., Voithknecht, U.C., Soll, J., and Westhoff, P.** (2001). VIPP1, a nuclear gene of *Arabidopsis thaliana* essential for thylakoid membrane formation. *Proc. Natl. Acad. Sci. USA* **98**: 4238–4242.
- Kusaba, M., Ito, H., Morita, R., Iida, S., Sato, Y., Fujimoto, M., Kawasaki, S., Tanaka, R., Hirochika, H., Nishimura, M., and Tanaka, A.** (2007). Rice NON-YELLOW COLORING1 is involved in light-harvesting complex II and grana degradation during leaf senescence. *Plant Cell* **19**: 1362–1375.
- Kuttkat, A., Edhofer, I., Eichacker, L.A., and Paulsen, H.** (1997). Light-harvesting chlorophyll a/b-binding protein stably inserts into etioplast membranes supplemented with Zn-pheophytin a/b. *J. Biol. Chem.* **272**: 20451–20455.
- Langdale, J.A., Rothermel, B., and Nelson, T.** (1988). Cellular patterns of photosynthetic gene expression in developing maize leaves. *Genes Dev.* **2**: 106–115.
- Larkin, R.M., Alonso, J.M., Ecker, J.R., and Chory, J.** (2003). GUN4, a regulator of chlorophyll synthesis and intracellular signaling. *Science* **299**: 902–906.
- Lascombe, M.-B., Bakan, B., Buhot, N., Marion, D., Blein, J.-P., Larue, V., Lamb, C., and Prange, T.** (2008). The structure of “defective in induced resistance” protein of *Arabidopsis thaliana*, DIR1, reveals a new type of lipid transfer protein. *Protein Sci.* **17**: 1522–1530.
- Lee, J., He, K., Stolz, V., Lee, H., Figueroa, P., Gao, Y., Tongprasit, W., Zhao, H., Lee, I., and Deng, X.W.** (2007). Analysis of transcription factor HY5 genomic binding sites revealed its hierarchical role in light regulation of development. *Plant Cell* **19**: 731–749.
- Martin, W., Rujan, T., Richly, E., Hansen, A., Cornelsen, S., Lins, T., Leister, D., Stoebe, B., Hasegawa, M., and Penny, D.** (2002). Evolutionary analysis of *Arabidopsis*, cyanobacterial, and chloroplast genomes reveals plastid phylogeny and thousands of cyanobacterial genes in the nucleus. *Proc. Natl. Acad. Sci. USA* **99**: 12246–12251.
- Matsumoto, F., Obayashi, T., Sasaki-Sekimoto, Y., Ohta, H., Takamiya, K.-i., and Masuda, T.** (2004). Gene expression profiling of the tetrapyrrole metabolic pathway in *Arabidopsis* with a mini-array system. *Plant Physiol.* **135**: 2379–2391.
- McCormac, A.C., Fischer, A., Kumar, A.M., Söll, D., and Terry, M.J.** (2001). Regulation of HEMA1 expression by phytochrome and a plastid signal during de-etiolation in *Arabidopsis thaliana*. *Plant J.* **25**: 549–561.
- Meng, X., Brodsky, M.H., and Wolfe, S.A.** (2005). A bacterial one-hybrid system for determining the DNA-binding specificity of transcription factors. *Nat. Biotechnol.* **23**: 988–994.
- Menkens, A.E., Schindler, U., and Cashmore, A.R.** (1995). The G-box: A ubiquitous regulatory DNA element in plants bound by the GBF family of bZIP proteins. *Trends Biochem. Sci.* **20**: 506–510.
- Meskauskiene, R., Nater, M., Goslings, D., Kessler, F., op den Camp, R., and Apel, K.** (2001). FLU: A negative regulator of chlorophyll biosynthesis in *Arabidopsis thaliana*. *Proc. Natl. Acad. Sci. USA* **98**: 12826–12831.
- Mochizuki, N., Brusslan, J.A., Larkin, R., Nagatani, A., and Chory, J.** (2001). *Arabidopsis* genomes uncoupled 5 (GUN5) mutant reveals the involvement of Mg-chelatase H subunit in plastid-to-nucleus signal transduction. *Proc. Natl. Acad. Sci. USA* **98**: 2053–2058.
- Mochizuki, N., Tanaka, R., Tanaka, A., Masuda, T., and Nagatani, A.** (2008). The steady-state level of Mg-protoporphyrin IX is not a determinant of plastid-to-nucleus signaling in *Arabidopsis*. *Proc. Natl. Acad. Sci. USA* **105**: 15184–15189.
- Monte, E., Tepperman, J.M., Al-Sady, B., Kaczorowski, K.A., Alonso, J.M., Ecker, J.R., Li, X., Zhang, Y., and Quail, P.H.** (2004). The phytochrome-interacting transcription factor, PIF3, acts early, selectively, and positively in light-induced chloroplast development. *Proc. Natl. Acad. Sci. USA* **101**: 16091–16098.
- Moon, J., Zhu, L., Shen, H., and Huq, E.** (2008). PIF1 directly and indirectly regulates chlorophyll biosynthesis to optimize the greening process in *Arabidopsis*. *Proc. Natl. Acad. Sci. USA* **105**: 9433–9438.
- Moran, R., and Porath, D.** (1980). Chlorophyll determination in intact tissues using N,N-dimethylformamide. *Plant Physiol.* **65**: 478–479.
- Moulin, M., McCormac, A.C., Terry, M.J., and Smith, A.G.** (2008). Tetrapyrrole profiling in *Arabidopsis* seedlings reveals that retrograde plastid nuclear signaling is not due to Mg-protoporphyrin IX accumulation. *Proc. Natl. Acad. Sci. USA* **105**: 15178–15183.
- Nakayama, K., Okawa, K., Kakizaki, T., Honma, T., Itoh, H., and Inaba, T.** (2007). *Arabidopsis* Cor15am is a chloroplast stromal protein that has cryoprotective activity and forms oligomers. *Plant Physiol.* **144**: 513–523.
- Oyama, T., Shimura, Y., and Okada, K.** (1997). The *Arabidopsis* HY5 gene encodes a bZIP protein that regulates stimulus-induced development of root and hypocotyl. *Genes Dev.* **11**: 2983–2995.
- Pavesi, G., Mereghetti, P., Mauri, G., and Pesole, G.** (2004). Weeder Web: Discovery of transcription factor binding sites in a set of sequences from co-regulated genes. *Nucleic Acids Res.* **32**: W199–203.
- Pfannschmidt, T., Brautigam, K., Wagner, R., Dietzel, L., Schroter, Y., Steiner, S., and Nykytenko, A.** (2009). Potential regulation of gene expression in photosynthetic cells by redox and energy state: approaches towards better understanding. *Ann. Bot. (Lond.)* **103**: 599–607.
- Pontier, D., Albrieux, C., Joyard, J., Lagrange, T., and Block, M.A.** (2007). Knock-out of the magnesium protoporphyrin IX

- methyltransferase gene in Arabidopsis: Effects on chloroplast development and on chloroplast-to-nucleus signaling. *J. Biol. Chem.* **282**: 2297–2304.
- Reed, J.W., Nagatani, A., Elich, T.D., Fagan, M., and Chory, J.** (1994). Phytochrome A and phytochrome B have overlapping but distinct functions in Arabidopsis development. *Plant Physiol.* **104**: 1139–1149.
- Reinbothe, C., Bartsch, S., Eggink, L.L., Hooper, J.K., Brusslan, J., Andrade-Paz, R., Monnet, J., and Reinbothe, S.** (2006). A role for chlorophyllide a oxygenase in the regulated import and stabilization of light-harvesting chlorophyll a/b proteins. *Proc. Natl. Acad. Sci. USA* **103**: 4777–4782.
- Riechmann, J.L., et al.** (2000). Arabidopsis transcription factors: Genome-wide comparative analysis among eukaryotes. *Science* **290**: 2105–2110.
- Rossini, L., Cribb, L., Martin, D.J., and Langdale, J.A.** (2001). The maize Golden2 gene defines a novel class of transcriptional regulators in plants. *Plant Cell* **13**: 1231–1244.
- Ruckle, M.E., DeMarco, S.M., and Larkin, R.M.** (2007). Plastid signals remodel light signaling networks and are essential for efficient chloroplast biogenesis in *Arabidopsis*. *Plant Cell* **19**: 3944–3960.
- Saleh, A., Alvarez-Venegas, R., and Avramova, Z.** (2008). An efficient chromatin immunoprecipitation (ChIP) protocol for studying histone modifications in Arabidopsis plants. *Nat. Protocols* **3**: 1018–1025.
- Savitch, L.V., Subramaniam, R., Allard, G.C., and Singh, J.** (2007). The GLK1 'regulon' encodes disease defense related proteins and confers resistance to *Fusarium graminearum* in Arabidopsis. *Biochem. Biophys. Res. Commun.* **359**: 234–238.
- Standfuss, J., Terwisscha van Scheltinga, A.C., Lamborghini, M., and Werner, K.** (2005). Mechanisms of photoprotection and non-photochemical quenching in pea light-harvesting complex at 2.5 Å resolution. *EMBO J.* **24**: 919–928.
- Stephenson, P.G., and Terry, M.J.** (2008). Light signalling pathways regulating the Mg-chelatase branchpoint of chlorophyll synthesis during de-etiolation in *Arabidopsis thaliana*. *Photochem. Photobiol. Sci.* **7**: 1243–1252.
- Strand, A., Asami, T., Alonso, J., Ecker, J.R., and Chory, J.** (2003). Chloroplast to nucleus communication triggered by accumulation of Mg-protoporphyrinIX. *Nature* **421**: 79–83.
- Sullivan, J.A., and Deng, X.W.** (2003). From seed to seed: The role of photoreceptors in Arabidopsis development. *Dev. Biol.* **260**: 289–297.
- Sun, C.-W., Chen, L.-J., Lin, L.-C., and Li, H.-m.** (2001). Leaf-specific upregulation of chloroplast translocon genes by a CCT motif-containing protein, CIA 2. *Plant Cell* **13**: 2053–2061.
- Sundqvist, C., and Dahlin, C.** (1997). With chlorophyll pigments from prolamellar bodies to light-harvesting complexes. *Physiol. Plant.* **100**: 748–759.
- Susek, R.E., Ausubel, F.M., and Chory, J.** (1993). Signal transduction mutants of Arabidopsis uncouple nuclear CAB and RBCS gene expression from chloroplast development. *Cell* **74**: 787–799.
- Tamai, H., Iwabuchi, M., and Meshi, T.** (2002). Arabidopsis GARP transcriptional activators interact with the Pro-rich activation domain shared by G-box binding bZIP factors. *Plant Cell Physiol.* **43**: 99–107.
- Tanaka, R., and Tanaka, A.** (2007). Tetrapyrrole biosynthesis in higher plants. *Annu. Rev. Plant Biol.* **58**: 321–346.
- Tepperman, J.M., Hwang, Y.-S., and Quail, P.H.** (2006). phyA dominates in transduction of red-light signals to rapidly responding genes at the initiation of Arabidopsis seedling de-etiolation. *Plant J.* **48**: 728–742.
- Terry, M.J., and Kendrick, R.E.** (1999). Feedback inhibition of chlorophyll synthesis in the phytochrome chromophore-deficient aurea and yellow-green-2 mutants of tomato. *Plant Physiol.* **119**: 143–152.
- Tompa, M., et al.** (2005). Assessing computational tools for the discovery of transcription factor binding sites. *Nat. Biotechnol.* **23**: 137–144.
- von Gromoff, E.D., Alawady, A., Meinecke, L., Grimm, B., and Beck, C.F.** (2008). Heme, a plastid-derived regulator of nuclear gene expression in *Chlamydomonas*. *Plant Cell* **20**: 552–567.
- Walters, R.G.** (2005). Towards an understanding of photosynthetic acclimation. *J. Exp. Bot.* **56**: 435–447.
- Walters, R.G., and Horton, P.** (1994). Acclimation of *Arabidopsis thaliana* to the light environment: Changes in composition of the photosynthetic apparatus. *Planta* **195**: 248–256.
- Walters, R.G., Rogers, J.J.M., Shephard, F., and Horton, P.** (1999). Acclimation of *Arabidopsis thaliana* to the light environment: the role of photoreceptors. *Planta* **209**: 517–527.
- Waters, M.T., Moylan, E.C., and Langdale, J.A.** (2008). GLK transcription factors regulate chloroplast development in a cell-autonomous manner. *Plant J.* **56**: 432–444.
- Weston, E., Thorogood, K., Vinti, G., and López-Juez, E.** (2000). Light quantity controls leaf-cell and chloroplast development in *Arabidopsis thaliana* wild type and blue-light-perception mutants. *Planta* **211**: 807–815.
- Workman, C.T., Yin, Y., Corcoran, D.L., Ideker, T., Stormo, G.D., and Benos, P.V.** (2005). enoLOGOS: A versatile web tool for energy normalized sequence logos. *Nucleic Acids Res.* **33**: W389–392.
- Yasumura, Y., Moylan, E.C., and Langdale, J.A.** (2005). A conserved transcription factor mediates nuclear control of organelle biogenesis in anciently diverged land plants. *Plant Cell* **17**: 1894–1907.
- Yi, X., Hargett, S.R., Frankel, L.K., and Bricker, T.M.** (2006). The PsbQ protein is required in Arabidopsis for photosystem II assembly/stability and photoautotrophy under low light conditions. *J. Biol. Chem.* **281**: 26260–26267.

**GLK Transcription Factors Coordinate Expression of the Photosynthetic Apparatus in
*Arabidopsis***

Mark T. Waters, Peng Wang, Muris Korkaric, Richard G. Capper, Nigel J. Saunders and Jane A. Langdale

Plant Cell 2009;21;1109-1128; originally published online April 17, 2009;
DOI 10.1105/tpc.108.065250

This information is current as of September 14, 2012

Supplemental Data	http://www.plantcell.org/content/suppl/2009/04/13/tpc.108.065250.DC1.html
References	This article cites 84 articles, 47 of which can be accessed free at: http://www.plantcell.org/content/21/4/1109.full.html#ref-list-1
Permissions	https://www.copyright.com/ccc/openurl.do?sid=pd_hw1532298X&issn=1532298X&WT.mc_id=pd_hw1532298X
eTOCs	Sign up for eTOCs at: http://www.plantcell.org/cgi/alerts/ctmain
CiteTrack Alerts	Sign up for CiteTrack Alerts at: http://www.plantcell.org/cgi/alerts/ctmain
Subscription Information	Subscription Information for <i>The Plant Cell</i> and <i>Plant Physiology</i> is available at: http://www.aspb.org/publications/subscriptions.cfm